

รายงานการวิจัย

เรื่อง

ฤทธิ์ต้านเบาหวาน กลไกการออกฤทธิ์ และความเป็นพิษ
ของ พี-เม็ททอกซี-ซินนามิค แอซิด
(Antidiabetic effects, mechanisms of action and toxicity
test of *p*-methoxy-*trans*-cinnamic acid)

(งบประมาณ ปี พ.ศ. 2550)

โดย

รศ.สพ.ญ.ดร. ศิรินทร หยิบไชคองหนัด
ภาควิชา เภสัชวิทยา คณะสัตวแพทยศาสตร์

รศ.น.สพ.ดร. วิจิตร บรรรลุนาร่า
ภาควิชา พยาธิวิทยา คณะสัตวแพทยศาสตร์

อ.ดร. สิริชัย อติศักดิ์วัฒนา
ภาควิชาเวชศาสตร์การธนาคารเลือด คณะสหเวชศาสตร์
จุฬาลงกรณ์มหาวิทยาลัย

ACKNOWLEDGEMENT

This research work is financially supported by Government Research Budget year 2006-2007.

บทคัดย่อ

คณะผู้วิจัยได้ทำการศึกษาฤทธิ์ของ พี-เม็ททอกซี ซินนามิค แอซิด (พี-เอ็มซีเอ) ซึ่งเป็นอนุพันธ์ชนิดหนึ่งของกรดซินนามิคในการลดระดับน้ำตาลในกระแสเลือด ผลต่อระดับฮอร์โมนอินซูลิน กลไกการออกฤทธิ์ในระดับเซลล์ การยับยั้งการทำงานของเอนไซม์ที่เกี่ยวข้องกับการย่อยคาร์โบไฮเดรต รวมทั้งศึกษาพิษเฉียบพลันของพี-เอ็มซีเอ ซึ่งพบว่า พี-เอ็มซีเอสามารถกระตุ้นการหลั่งอินซูลินจากการผ่านสารดังกล่าวเข้าสู่ตับอ่อนโดยตรง รวมทั้งกระตุ้นการหลั่งอินซูลินจากเซลล์ไอเอ็นเอสวันตามความเข้มข้นที่เพิ่มขึ้น นอกจากนี้พี-เอ็มซีเอเพิ่มระดับความเข้มข้นของแคลเซียมภายในเซลล์ไอเอ็นเอสวัน การกระตุ้นการหลั่งอินซูลินและการเพิ่มระดับแคลเซียมภายในเซลล์ของพี-เอ็มซีเอนั้นถูกยับยั้งในภาวะการขาดแคลเซียมภายนอกเซลล์และภาวะที่มีโมดิฟิโนซึ่งเป็นแอลไทป์แคลเซียมชาแนลแอนตาโกนิสต์ จากผลการทดลองดังกล่าวกลไกของพี-เอ็มซีเอในการกระตุ้นการหลั่งอินซูลิน เกี่ยวข้องกับการเหนี่ยวนำแคลเซียมเข้าสู่เซลล์โดยผ่านทางแอลไทป์-แคลเซียมชาแนล ไดอะซอกไซด์ไม่สามารถยับยั้งกลไกของพี-เอ็มซีเอดังกล่าวในการกระตุ้นการหลั่งอินซูลินและเพิ่มระดับแคลเซียมภายในเซลล์ นอกจากนี้พี-เอ็มซีเอยังเพิ่มฤทธิ์ของกลูโคสและไกลบูลูไรต์และเสริมฤทธิ์ของโปแตสเซียมคลอไรด์ และแคลเซียมชาแนล ชนิดแอลไทป์ในการหลั่งอินซูลินและเพิ่มระดับแคลเซียมภายในเซลล์ พี-เอ็มซีเอสามารถเพิ่มระดับไซคลิก-เอเอ็มพีภายในเซลล์รวมทั้งเสริมฤทธิ์ของฟออสโคลินซึ่งเป็นตัวกระตุ้นการทำงานของเอนไซม์อะดีนาลิไซเคส แต่อย่างไรก็ตาม พี-เอ็มซีเอไม่สามารถเพิ่มไซคลิก-เอเอ็มพีในกรณีที่กระตุ้นด้วยสามไอโซบิวทิลวันเมทิลแซนทีน พี-เอ็มซีเอสามารถยับยั้งการทำงานของเอนไซม์อัลฟาไกลูโคซิเดสจากยีสต์ด้วยกลไกแบบแข่งขันได้แต่ไม่สามารถยับยั้งเอนไซม์ดังกล่าวจากสัตว์เลี้ยงลูกด้วยนมและเอนไซม์อัลฟาอะไมเลสได้

จากการทดสอบพิษเฉียบพลันของพี-เอ็มซีเอ พบว่า พี-เอ็มซีเอไม่มีผลทำให้สัตว์ทดลองตายที่ความเข้มข้น 100 ถึง 2,000 มก./กก. เมื่อตรวจค่าชีวเคมีทางเลือดของหนูที่ได้รับ พี-เอ็มซีเอพบว่าค่าดังกล่าวไม่แตกต่างกับกลุ่มควบคุมที่ได้รับการป้อนน้ำมันดอกทานตะวัน รวมทั้งไม่พบความแตกต่างทางพยาธิวิทยาของสมอง ตับอ่อน หัวใจ และปอดในหนูทั้งสองกลุ่ม

ABSTRACT

p-Methoxycinnamic acid (*p*-MCA) is a cinnamic acid derivative that shows various pharmacologic actions such as neuroprotective and hepatoprotective activities. To examine the insulinotropic activity of *p*-MCA, the perfused rat pancreas and a pancreatic β -cell line, INS-1 were used in the studies. *p*-MCA increased insulin secretion from the perfused rat pancreas and INS-1 cells in a concentration-dependent manner. In addition, *p*-MCA increased intracellular Ca^{2+} concentration ($[\text{Ca}^{2+}]_i$) in INS-1 cells. The *p*-MCA-induced insulin secretion and rise in $[\text{Ca}^{2+}]_i$ were markedly inhibited in the absence of extracellular Ca^{2+} or in the presence of an L-type Ca^{2+} channel blocker, nimodipine. These results suggested that *p*-MCA increased Ca^{2+} influx via the L-type Ca^{2+} channels. Diazoxide, an ATP-sensitive K^+ channel opener, did not alter *p*-MCA-induced insulin secretion, nor $[\text{Ca}^{2+}]_i$ response. In addition, *p*-MCA enhanced glucose- and glyburide-induced insulin secretion and it also potentiated the increase in insulin secretion and a rise of $[\text{Ca}^{2+}]_i$ induced by KCl- and Bay K 8644, an L-type Ca^{2+} channel. Furthermore, *p*-MCA increased cyclic AMP content of INS-1 cells and enhanced the increase of cyclic AMP content induced by an adenylyl cyclase activator forskolin; however, *p*-MCA failed to enhance the effect of a phosphodiesterase inhibitor 3-isobutyl-1-methylxanthine. Taken together, our results suggested that *p*-MCA stimulated insulin secretion from pancreatic β -cells by increasing Ca^{2+} influx via the L-type Ca^{2+} channels, but not through the closure of ATP-sensitive K^+ channels. In addition, *p*-MCA may increase cyclic AMP content by inhibiting phosphodiesterase. *p*-MCA was a potent competitive inhibitor against yeast α -glucosidase. However, it had no inhibitory activities on mammalian α -glucosidases and α -amylase.

In the acute toxicity test, oral administration of *p*-MCA (100-2000 mg/kg) produced neither mortality nor significant differences in blood chemistry analysis when compared to the control group, which was fed with sunflower oil. In addition, neither gross abnormalities nor histopathological changes of brain, pancreas, heart and lung were observed.

CONTENTS

	Pages
ACKNOWLEDGEMENT.....	2
THAI ABSTRACT.....	3
ENGLISH ABSTRACT.....	4
LIST OF FIGURES.....	6
LIST OF TABLES.....	8
ABBREVIATIONS.....	9
CHAPTER	
I. INTRODUCTION.....	10
II. MATERIALS AND METHODS.....	11
III. RESULTS.....	18
IV. DISCUSSION & CONCLUSION	50
REFERENCES.....	55

LIST OF FIGURES

Figure		page
1	Effect of <i>p</i> -MCA on insulin secretion from perfused rat pancreas	19
2	Effect of <i>p</i> -MCA on insulin secretion in INS-1 cells	20
3	Concentration-dependent effect of <i>p</i> -MCA on $[Ca^{2+}]_i$ increase in INS-1 cells	21
4	Effect of <i>p</i> -MCA on insulin secretion in INS-1 cells in presence of Ca^{2+} free KRB or Nimodipine	26
5	Effect of <i>p</i> -MCA on $[Ca^{2+}]_i$ in the presence of Ca^{2+} free KRB and nimodipine	27
6	Effect of <i>p</i> -MCA and glyburide on insulin secretion in INS-1 cells in presence of diazoxide	28
7	Effect of <i>p</i> -MCA on $[Ca^{2+}]_i$ response in presence of diazoxide	29
8	Effect of <i>p</i> -MCA on glucose-induced insulin secretion in perfused rat pancreas	30
9	Effect of <i>p</i> -MCA on glucose-induced insulin secretion in INS-1 cells	31
10	Effect of <i>p</i> -MCA on glucose-induced $[Ca^{2+}]_i$ increase	32
11	Effect of <i>p</i> -MCA on insulin secretion in INS-1 cells in presence of glyburide	33
12	Effect of <i>p</i> -MCA on glyburide-induced $[Ca^{2+}]_i$ increase	34
13	Effect of <i>p</i> -MCA on insulin secretion in INS-1 cells in presence of KCl	35
14	Effect of <i>p</i> -MCA on KCl-induced $[Ca^{2+}]_i$ increase	36
15	Effect of <i>p</i> -MCA on insulin secretion in INS-1 cells in presence of Bay K 8644	37
16	Effect of <i>p</i> -MCA on Bay K 8644-induced insulin secretion in perfused rat pancreas	38
17	Effect of <i>p</i> -MCA on Bay K 8644-induced $[Ca^{2+}]_i$ increase	39
18	Effect of <i>p</i> -MCA on insulin secretion in INS-1 cells in presence of forskolin	40
19	Effect of <i>p</i> -MCA on insulin secretion in INS-1 cells in presence of IBMX	41

20	Lineweaver-burk plot analysis of the inhibition kinetics of α -glucosidase inhibitory effects by <i>p</i> -MCA	45
21	Mild degree of fat accumulation in the renal tubules of the kidneys	47
22	Moderate glycogen degeneration with the presence of hyaline droplets in the cytoplasm of the renal tubules	48
23	Mild degree of fatty degeneration of liver	48
24	Moderate diffuse panlobular glycogen degeneration of liver	49

LIST OF TABLES

Table	page
1 Effects of <i>p</i> -MCA on cAMP concentrations in INS-1 cells in presence of forskolin and IBMX	42
2 In vitro studies of inhibitory effect of <i>p</i> -MCA on α -glucosidase, pancreatic lipase, and α -amylase	44

ABBREVIATIONS

IDDM	=	Insulin-Dependent Diabetes Mellitus
NIDDM	=	Noninsulin-Dependent Diabetes mellitus
FBP	=	fasting plasma glucose
PPG	=	postprandial plasma glucose
<i>p</i> -MCA	=	<i>p</i> -methoxycinnamic acid
STZ	=	streptozotocin
°C	=	degree celsius
mmol/l	=	milimolar
M	=	molar
μM	=	micromolar
g	=	gram
kg	=	kilogram
mg	=	miligram
ml	=	milliliter
μl	=	microlitre
dl	=	deciliter
PEPCK	=	phosphoenolpyruvate carboxykinase
SUR	=	sulfonylurea receptor
NMDA	=	N-methyl-D-aspartate
NB-DNJ	=	N-butyldeoxynojirimycin
KRB	=	Krebs-Ringer bicarbonate buffer

INTRODUCTION

Insulin secretion from β -cells is principally regulated by plasma glucose concentrations. After being transported into the cell, glucose is metabolized via glycolysis, tricarboxylic acid cycle, and oxidative phosphorylation, resulting in an increase in ATP production. The rise of cytosolic ATP/ADP ratio in the β -cells leads to the closure of the ATP-sensitive K^+ channels (K_{ATP} channels), evoking membrane depolarization, and subsequent activation of the voltage-dependent Ca^{2+} channels (VDCCs). This permits the opening of VDCCs and an increase in $[Ca^{2+}]_i$, which triggers the fusion of insulin-containing secretory vesicles to the plasma membrane, and exocytosis of insulin follows rapidly (Ashcroft, 2005). Sulfonylureas are the compounds that directly stimulate insulin secretion from pancreatic β -cells (Rajan et al., 1990); they are used to treat patients with type 2 diabetes. However, sulfonylureas can produce hypoglycemia, and secondary failure of insulin secretion (Jackson and Bressler, 1981; Ferner and Neil, 1988; Gerich, 1989; Jennings et al., 1989), which may be due to β -cells exhaustion resulting from over-stimulation. Great efforts have been put forth to search for insulinotropic agents for the control of type 2 diabetes.

Cinnamic acid and its derivatives possess a variety of pharmacologic properties, including hepatoprotective (Perez-Alvarez et al., 2001), anti-malarial (Wiesner et al., 2001), antioxidant (Natella et al., 1999), and antihyperglycemic activities (Liu et al., 1999). In addition, 4-hydroxy-3-methoxycinnamic acid (ferulic acid) and amides compounds derived from ferulic acid increase insulin secretion in RIN-5F cells (Nomura et al., 2003).

p-Methoxycinnamic acid (*p*-MCA), a cinnamic acid derivative, was isolated from the roots of *Scrophularia buergeriana* (Kim et al., 2003) and the leaves with stems of *Aquilegia vulgaris* (Bylka, 2004). The compound has attracted considerable interest in recent years due to its various pharmacologic activities. For examples, *p*-MCA has hepatoprotective activity in CCl_4 -induced toxicity in rat hepatocytes (Lee et al., 2002). It also exerts protective effect against glutamate-induced degeneration in cortical neurons (Kim et al., 2002). Our previous study demonstrated that *p*-MCA was a non-competitive α -glucosidase inhibitor and exhibited the most potent inhibitory activity among the

cinnamic acid derivatives studied (Adisakwattana et al., 2004). We have recently reported the antihyperglycemic activity of *p*-MCA in normal and streptozotocin-induced diabetic rats (Adisakwattana et al., 2005). In that study, *p*-MCA markedly reduced hyperglycemia in diabetic rats by increasing activity of glycolytic enzymes and inhibiting gluconeogenic enzymes. However, insulinotropic properties of *p*-MCA have not been reported. The aim of the present study was to determine whether *p*-MCA stimulates insulin secretion. In addition, the study was undertaken to elucidate the mechanisms underlying *p*-MCA-induced insulin secretion.

MATERIALS AND METHODS

1. The pancreatic perfusion

Male rats were anesthetized with pentobarbital sodium (60 mg/kg ip) and were maintained at 37°C on a hot plate during the experiment. The celiac arteries were cannulated with polyvinyl tubing, and then the pancreata were immediately perfused with the Krebs-Ringer Bicarbonate buffer (KRB) supplemented with 20 mM HEPES, 5.5 mM glucose, 1% dextran, and 0.2% bovine serum albumin (BSA) as a basal medium. The KRB was continuously aerated with 95% O₂-5% CO₂ at pH 7.4. The perfusion rate was 1 ml/min, and the effluent fluid from the portal vein, which was cannulated with a vinyl tubing, was ~1 ml/min. The rats were euthanized immediately after the placement of cannulas and the beginning of the flow. The perfused pancreas was equilibrated for 20 min before the onset of the experiment. The pancreatic perfusions were performed in three different experiments. For the first study, after the baseline period of 10 min, the perfusate containing *p*-MCA (10 μM or 100 μM) was administered for 30 min followed by a washout period with the basal medium for 10 min. The perfusate containing glucose (10 mM) was administered as a positive control for 10 min at the end of the experiments. For the second study, after the baseline period of 10 min, the perfusate containing 10 mM glucose was administered for 20 min and followed by glucose with or without 10 μM *p*-MCA for 20 min. For the third study, after

the baseline period of 10 min, the perfusate containing 1 μM Bay K 8644 (L-type Ca^{2+} channel agonist) with or without 10 μM *p*-MCA was administered for 30 min. (Yibchok-anun et al., 1998).

2. Cell culture

INS-1 cells, an insulin-secreting cell line derived from rat pancreatic β -cells were cultured in RPMI 1640 medium containing 11 mM glucose and supplemented with 10% fetal bovine serum, 2 mM L-glutamine, 1 mM sodium pyruvate and 50 μM 2-mercaptoethanol in an atmosphere of 5% CO_2 in air at 37°C.

3. Insulin Secretion Studies

INS-1 Cells were plated onto 24-well plates at a density of 1×10^5 cells per well and grown for 48 h. For static secretion studies, cells were preincubated for 15 min in KRB containing 4 mM glucose and 0.1% BSA. Cells were then incubated for 30 min in KRB containing test agents.

Experiment 1. Dose dependency study: The cells were incubated with various concentrations of *p*-MCA (1 – 300 μM).

Experiment 2. The cells were incubated with 100 μM *p*-MCA in Ca^{2+} free KRB or 1 μM Nimodipine (L-type Ca^{2+} channel blocker).

Experiment 3. The cells were incubated with 100 μM *p*-MCA in presence of 400 μM diazoxide (K_{ATP} channel opener). 10 μM glyburide was used as a positive control for this study.

Experiment 4. The cells were incubated with 10 mM glucose for 15 min and then *p*-MCA (10 or 100 μM) was added to the cells for 15 min.

Experiment 5. The cells were incubated with *p*-MCA (10 or 100 μM) in presence of 15 mM KCl.

Experiment 6. The cells were incubated with *p*-MCA (10 or 100 μM) in presence of 1 μM Bay K 8644 (L-type Ca^{2+} channel agonist).

Experiment 7. The cells were incubated with *p*-MCA (10 or 100 μM) in presence of 10 μM glyburide.

Experiment 8. The cells were incubated with *p*-MCA (10 or 100 μM) in presence of 1 μM forskolin (adenylyl cyclase activator). After incubation, the cell were determined for the cAMP contents.

Experiment 9. The cells were incubated with *p*-MCA (10 or 100 μM) in presence of 100 μM IBMX (phosphodiesterase inhibitor). After incubation the cell were determined for the cAMP contents.

After incubation, the buffer was kept at 4°C and subsequently assayed for insulin. *p*-MCA was dissolved in dimethyl sulfoxide (DMSO) to obtain desired concentrations (final concentration, 0.2%).

4. Measurement of $[\text{Ca}^{2+}]_i$

Cells were grown in culture flasks for 5 days until 80–90% confluence had been reached. Thereafter, the cells were harvested by treatment with trypsin/EDTA and prepared for experiments. Measurement of $[\text{Ca}^{2+}]_i$ was accomplished by loading cells with 2 μM fura 2-AM (Fura-2 acetoxymethylester) for 30min at 37°C in KRB. The loaded cells were centrifuged at 300xg for 2 min and resuspended with KRB. The 340/380nm fluorescence ratios were monitored using a spectrofluorometer (USA.). The $[\text{Ca}^{2+}]_i$ was calibrated as described previously (Cheng et al., 2005).

Experiment 1. Dose dependency study: Baseline was run for 60 second, then the various concentrations of *p*-MCA (1 – 300 μM) were added to the cells.

Experiment 2. Experiments in Ca^{2+} -free medium were done by centrifugation at 300g for 60s followed by resuspension of the cells in Ca^{2+} -free KRB containing 100 μM EGTA. In presence of Ca^{2+} free KRB, baseline was run for 60 seconds, then 100 μM *p*-MCA was added to the cells. After 120 seconds, 1 μM thapsigargin was added to the cells.

Experiment 3. Baseline was run for 60 seconds, then 1 μM Nimodipine was added to the cells. After 120 seconds, 100 μM *p*-MCA was added to the cells. Finally, 1 μM Bay K 8644 was added to the cells after 120 seconds of adding *p*-MCA

Experiment 4. Baseline was run for 60 seconds, then 400 μM diazoxide was added to the cells. 100 μM *p*-MCA was added to the cells after 120 seconds adding of diazoxide.

Experiment 5. Baseline was run for 60 seconds, then 10 mM glucose was added to the cells. 10 or 100 μM *p*-MCA was added to the cells after 120 seconds adding of glucose.

Experiment 6. Baseline was run for 60 seconds, then 15 mM KCl was added to the cells. 10 or 100 μM *p*-MCA was added to the cells after 120 seconds adding of KCl.

Experiment 7. Baseline was run for 60 seconds, then 1 μM Bay K 8644 was added to the cells. 10 or 100 μM *p*-MCA was added to the cells after 120 seconds adding of Bay K 8644.

Experiment 8. Baseline was run for 60 seconds, then 10 μM glyburide was added to the cells. 10 or 100 μM *p*-MCA was added to the cells after 120 seconds adding of glyburide.

5. cAMP determination

Cells were incubated with *p*-MCA (10 or 100 μM) in presence of 1 μM forskolin or 100 μM IBMX for 30 min. After remove the KRB solution, the cells were homogenized with 0.1 M HCl and the cells were scraped off. The cells were incubated in the water at

70°C. After incubation, the cell were centrifuged at 2,000g at 4 °C for 10 min and the supernatant was neutralized with 0.1 M NaOH. The solution was added the acetylating reagent (0.5 ml of acetic anhydride and 1 ml of triethylamine) and determined the cAMP level by using radioimmunoassay as previously described (Praong et al., 2001).

6. Microbial and mammalian α -glucosidase inhibition

Briefly, α -glucosidase from baker's yeast was assayed using 0.1 M phosphate buffer at pH 6.9, and 1 mM *p*-nitrophenyl- α -D-glucopyranoside (PNP-G) was used as a substrate. The concentration of the enzymes were 1 U/ml in each experiment. Forty microlitre of α -glucosidase was incubated in the absence or presence of various concentrations of *p*-MCA (10 μ l) at 37°C. The preincubation time was specified at 10 min and PNP-G solution (950 μ l) was added to the mixture. The reaction was carried out at 37 °C for 20 min, and then 1 ml of 1 M Na₂CO₃ was added to terminate the reaction. Enzymatic activity was quantified by measuring the absorbance at 405 nm. One unit of α -glucosidase is defined as the amount of enzyme liberating 1.0 μ mol of PNP per minute under the conditions specified. 1-Deoxynorjirimycin was used as the positive control in this study. In order to evaluate the type of inhibition using the Lineweaver-Burk plot, the enzyme reaction was performed according to the above reaction with various concentrations of *p*-MCA and PNP-G (Mutsui et al., 1996). The IC₅₀ values was expressed as mean \pm SE; n=3.

α -glucosidase from intestinal mammalian was assayed according to the method of Toda (2000). Briefly, rat intestinal acetone powder (100 mg) was homogenized in 3 ml of 0.9% NaCl solution. After centrifugation at 12,000xg for 30 min, 10 μ l of the supernatant was incubated with 70 μ l of substrate solution (37 mM maltose, 56 mM sucrose), and 20 μ l of *p*-MCA at various concentrations in 0.01 M phosphate buffer saline pH 6.9 at 37 °C for 30 min (maltase assay) and 60 min (sucrase assay). The concentrations of glucose released from the reaction mixtures were determined by using glucose oxidase method. Acarbose was used as the positive control in this study The IC₅₀ values were expressed as mean \pm SE; n=3.

70°C. After incubation, the cell were centrifuged at 2,000g at 4 °C for 10 min and the supernatant was neutralized with 0.1 M NaOH. The solution was added the acetylating reagent (0.5 ml of acetic anhydride and 1 ml of triethylamine) and determined the cAMP level by using radioimmunoassay as previously described (Praong et al., 2001).

6. Microbial and mammalian α -glucosidase inhibition

Briefly, α -glucosidase from baker's yeast was assayed using 0.1 M phosphate buffer at pH 6.9, and 1 mM *p*-nitrophenyl- α -D-glucopyranoside (PNP-G) was used as a substrate. The concentration of the enzymes were 1 U/ml in each experiment. Forty microlitre of α -glucosidase was incubated in the absence or presence of various concentrations of *p*-MCA (10 μ l) at 37°C. The preincubation time was specified at 10 min and PNP-G solution (950 μ l) was added to the mixture. The reaction was carried out at 37 °C for 20 min, and then 1 ml of 1 M Na₂CO₃ was added to terminate the reaction. Enzymatic activity was quantified by measuring the absorbance at 405 nm. One unit of α -glucosidase is defined as the amount of enzyme liberating 1.0 μ mol of PNP per minute under the conditions specified. 1-Deoxynorjirimycin was used as the positive control in this study. In order to evaluate the type of inhibition using the Lineweaver-Burk plot, the enzyme reaction was performed according to the above reaction with various concentrations of *p*-MCA and PNP-G (Mutsui et al., 1996). The IC₅₀ values was expressed as mean \pm SE; n=3.

α -glucosidase from intestinal mammalian was assayed according to the method of Toda (2000). Briefly, rat intestinal acetone powder (100 mg) was homogenized in 3 ml of 0.9% NaCl solution. After centrifugation at 12,000xg for 30 min, 10 μ l of the supernatant was incubated with 70 μ l of substrate solution (37 mM maltose, 56 mM sucrose), and 20 μ l of *p*-MCA at various concentrations in 0.01 M phosphate buffer saline pH 6.9 at 37 °C for 30 min (maltase assay) and 60 min (sucrase assay). The concentrations of glucose released from the reaction mixtures were determined by using glucose oxidase method. Acarbose was used as the positive control in this study The IC₅₀ values were expressed as mean \pm SE; n=3.

7. α -amylase inhibition

Pancreatic porcine α -amylase was dissolved in 0.1 M phosphate buffer saline, pH 6.9. *p*-MCA was added to solution containing in 1g/l starch and phosphate buffer. The reaction was initiated by adding amylase (1U/ml) to the incubation medium to a final volume of 150 μ l. After 10 min the reaction was stopped by adding 1 ml dinitrosalicylic (DNS) reagent (1% 3,5-dinitrosalicylic acid, 0.2% phenol, 0.05% Na₂SO₃, and 1% NaOH in aqueous solution) to the reaction mixture. The capped test tubes were heated at 100 °C for 15 min to develop the yellow-brown colour. After then 300 μ l of a 40% potassium sodium tartarate (Rochelle salt) solution was added to the test tubes to stabilize the color. After cooling to room temperature in a cold water bath, absorbance was recorded at 540 nm using spectrophotometer (Kanda et al., 2005). Acarbose was used as the positive control in this study. The IC₅₀ values were expressed as mean \pm SE; n=3.

Calculation of the percent inhibition and IC₅₀ values

$$\% \text{ Inhibitory activity} = \frac{(A_c - A_t)}{A_c} \times 100$$

A_c = Absorbance of control

A_t = Absorbance of test samples

IC₅₀ values were determined from plots of concentration vs percent inhibition curves using Sigma Plot 8.0.

8. Acute toxicity test

Normal mice were randomly divided into 6 groups of five animals per sex. Group 1 orally received distilled water. Group 2 received sunflower oil (vehicle). Group 3-5 received *p*-MCA at 100, 1,000 and 2,000 mg/kg. Signs of toxicity and mortality were observed after the administration at the first, second, fourth and sixth hour and once daily for 14 days. On the day 15, all rats were fasted for 16–18 h, then sacrificed for

necropsy examination. The internal organs were excised and weighed. The gross pathological observations of the tissues were performed. All mice were fasted overnight and blood samples were collected at 9 a.m. for determination of fasting plasma glucose, blood nitrogen urea (BUN), alanine aminotransferase (ALT), aspartate aminotransferase (AST), cholesterol, triglycerides and high-density lipoprotein (HDL) cholesterol and complete blood count (CBC).

9. Histological studies

Mice were sacrificed, and then pancreas, kidney, and liver were removed and immediately immersed in 10% formalin. After embedding, thick sections were prepared and stained with hematoxylin and eosin. All tissues were serially sectioned and the sections were determined under light microscope. The liver and kidney samples were stained with Periodic acid-Schiff reaction (PAS) for demonstration of the polysaccharides.

9. Data analysis

Data are expressed as means \pm S.E.M. Area under the curve (AUC) values are reported as total areas and are calculated using a modification of the trapezoidal rule. In animal models, statistical analysis was performed by 1) one-way analysis of variance (ANOVA) in the dose-response experiments, and 2) two-way ANOVA with a factorial design (diabetes x treatment). In the data from perfusion experiments, areas under the curve (AUCs) for the treatment period were calculated using Transforms and Regressions (SigmaPlot 8.0; SPSS, Chicago, IL) and expressed as a percentage of the area of the basal control group. The Least Significant Difference test was used for mean comparisons; $P < 0.05$ was considered to be statistically significant.

RESULTS

1. Effects of *p*-MCA on insulin secretion

The results in Fig 1 show the profile of *p*-MCA on insulin secreted from perfused rat pancreata and INS-1 cells. *p*-MCA (10 and 100 μM) increased insulin secretion from the perfused rat pancreata to 1.4 and 3.1 times of the basal control group, respectively (Fig 1). The effluent insulin concentrations returned to the baseline during the washout period, and increased to 6 times of the baseline value upon administration of 10 mM glucose. By calculating the percentage of AUC of the control group, *p*-MCA significantly increased insulin secretion when compared with the corresponding the control group (control = 100%; 10 μM *p*-MCA = $142.4 \pm 22.1\%$; 100 μM *p*-MCA = $314.6 \pm 15.6\%$). *p*-MCA (30 – 300 μM) also increased insulin secretion from INS-1 cells in a concentration-dependent manner (Fig 2). From cytotoxicity testing by MTT assay demonstrated that *p*-MCA (100 μM) did not affect cell viability of INS-1 cells, suggesting that *p*-MCA is not acutely toxic to this β -cell line.

2. Effects of *p*-MCA on $[\text{Ca}^{2+}]_i$ of INS-1 Cells

Since Ca^{2+} is an important intracellular signal, and it mediates the effect of many insulin secretagogues, the experiments were next performed to determine the effect of *p*-MCA on $[\text{Ca}^{2+}]_i$ in INS-1 cells, and the results of these experiments are shown in Fig 3. *p*-MCA (10-100 μM) increased $[\text{Ca}^{2+}]_i$ in a concentration-dependent manner. *p*-MCA-induced $[\text{Ca}^{2+}]_i$ increase reached maximum within 60 s of administration, which was followed by a small sustained phase. At 10 and 30 μM *p*-MCA, the $\Delta [\text{Ca}^{2+}]_i$ increases were 23 ± 1 nM and 40 ± 2 nM above the basal level, respectively. Exposure of cells to 100 μM *p*-MCA induced a larger increase in $\Delta[\text{Ca}^{2+}]_i$ of 63 ± 3 nM over the basal level. The results suggested that *p*-MCA-stimulated insulin secretion was associated with a rise in $[\text{Ca}^{2+}]_i$.

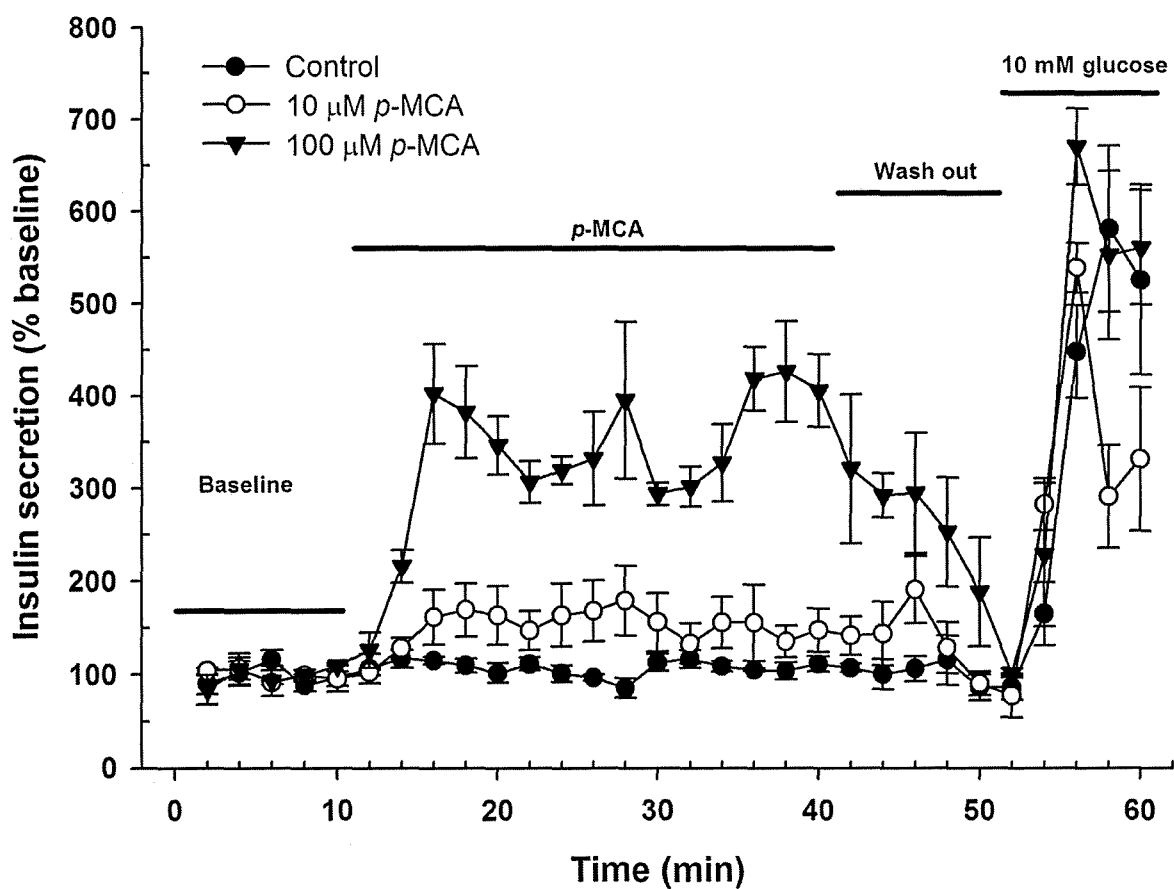


Figure 1 Effect of *p*-MCA (10 and 100 μ M) on insulin secretion from perfused rat pancreas. In these experiments, a 20-min equilibration period preceded *time 0*. *p*-MCA was administered for 30 min. Values are means \pm S.E.M.; $n = 3$, pancreata. Range of baseline insulin concentrations of effluents was 1.7 – 3.6 ng/ml.

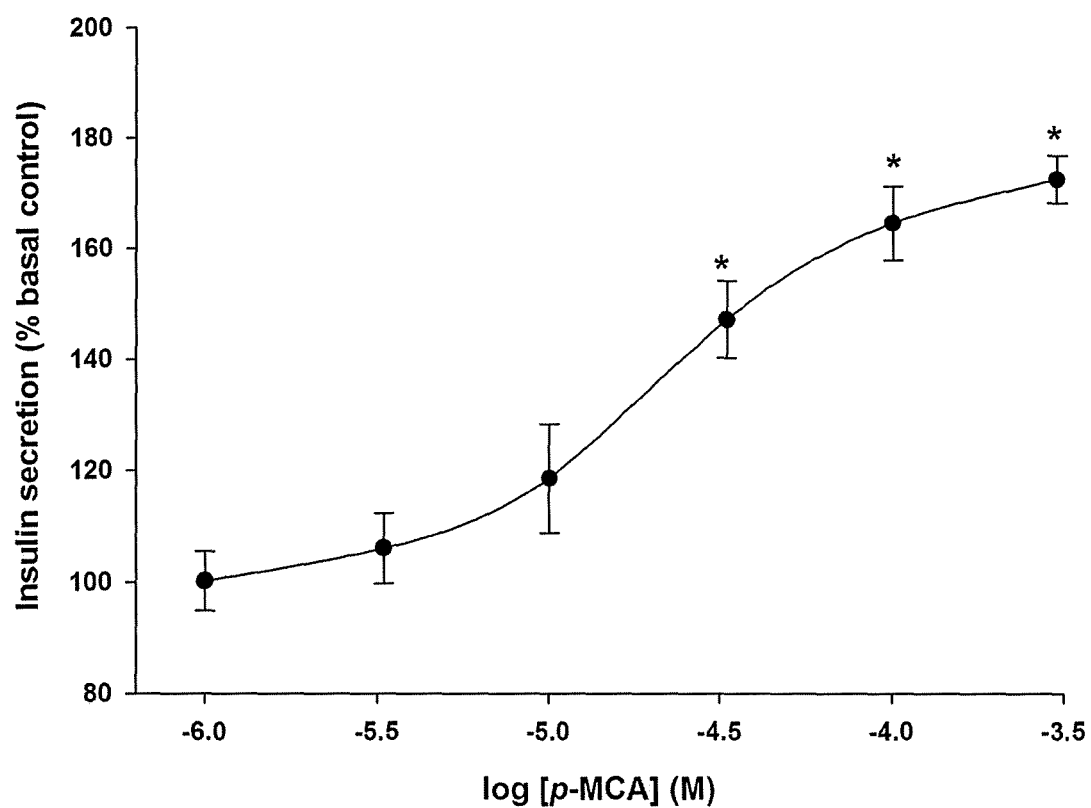


Figure 2. Effect of *p*-MCA on insulin secretion in INS-1 cells. The cells were preincubated for 15 min in KRB containing 4 mM glucose and 0.1% BSA. Cells were then incubated for 30 min in various concentrations of *p*-MCA. The control group had 3.54 ± 1.19 ng/well/ 30 min. Data are expressed as means \pm S.E.M.; $n=3$ independent experiments with quadruplicates in each experiment. * $P < 0.05$ vs. control group.

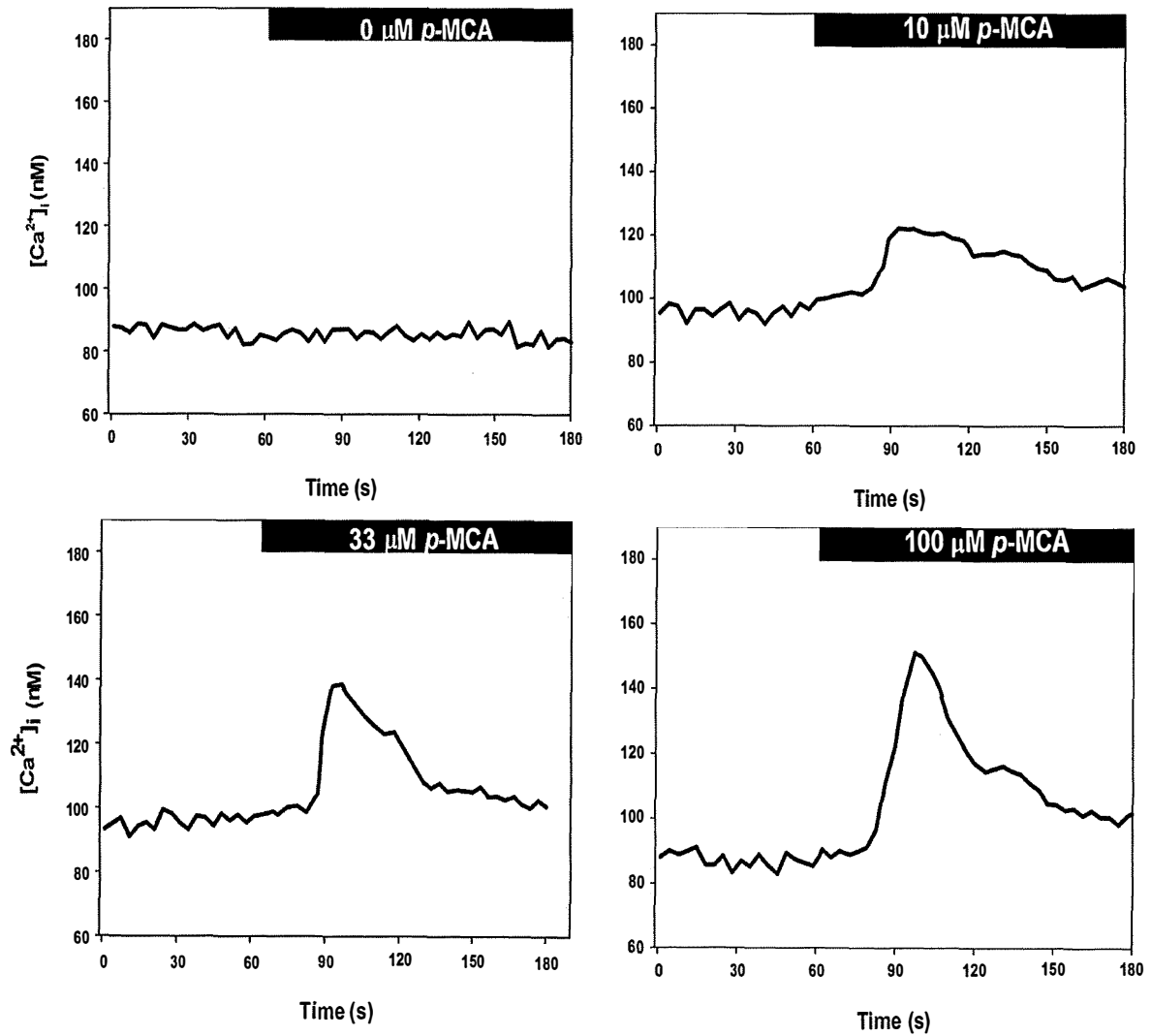


Figure 3. Concentration-dependent effect of *p*-MCA on $[Ca^{2+}]_i$ increase in INS-1 cells; (A) control group (B) 10 μ M *p*-MCA, (C) 33 μ M *p*-MCA, and (D) 100 μ M *p*-MCA. Traces are representative of 4 independent experiments with 20 cells/experiment.

3. Effect of *p*-MCA-induced insulin secretions and $[Ca^{2+}]_i$ responses under a Ca^{2+} -free condition or in the presence of an L-type Ca^{2+} channel antagonist.

The roles of extracellular Ca^{2+} and VDCC in *p*-MCA-stimulated insulin secretion were examined using extracellular Ca^{2+} -free solution containing 0.1 mM EGTA, or an L-type Ca^{2+} channel blocker (nimodipine) in the presence of extracellular Ca^{2+} (Fig 4). In the Ca^{2+} containing KRB, *p*-MCA (100 μ M) significantly increased insulin secretion by 60% in INS-1 cells over the basal control. The extracellular Ca^{2+} -free condition decreased basal insulin secretion when compared with Ca^{2+} -containing KRB. The results showed that *p*-MCA failed to increase insulin secretion in the absence of extracellular Ca^{2+} , and 1 μ M nimodipine significantly blocked the secretory response to *p*-MCA. In the β -cells that were under the Ca^{2+} -free condition (Fig 5A.), basal $[Ca^{2+}]_i$ were lower than those in Ca^{2+} -containing KRB. Under this circumstances, *p*-MCA failed to increase $[Ca^{2+}]_i$, whereas 1 μ M thapsigargin, an endoplasmic reticulum Ca^{2+} -ATPase inhibitor, caused the rise in $[Ca^{2+}]_i$. Figure 5B shows that $[Ca^{2+}]_i$ response to *p*-MCA was abolished by 1 μ M nimodipine, which also blocked Bay K 8644-stimulated $[Ca^{2+}]_i$ elevation. In addition, 1 μ M nimodipine alone did not significantly change the basal $[Ca^{2+}]_i$ or insulin secretion. These findings are consistent with those of insulin secretion studies.

4. Effects of *p*-MCA on insulin secretion and $[Ca^{2+}]_i$ response in the presence of a K_{ATP} channel opener

To determine whether *p*-MCA increases insulin secretion by closing K_{ATP} channels, *p*-MCA was incubated with diazoxide, a K_{ATP} channel opener. As shown in Fig. 6, diazoxide (400 μ M) did not affect the basal insulin concentration in the presence of 4 mM glucose. Glyburide (10 μ M), a K_{ATP} channel antagonist, significantly increased insulin secretion by ~2.0-fold, whereas its stimulatory effect was virtually abolished in the presence of diazoxide. In contrast, diazoxide did not block the effect of *p*-MCA-induced insulin secretion. The *p*-MCA-induced increase in $[Ca^{2+}]_i$ in the presence of diazoxide is shown in Fig. 7 It was found that diazoxide did not change the basal $[Ca^{2+}]_i$ in INS-1 cells. Meanwhile, diazoxide failed to inhibit *p*-MCA-induced $[Ca^{2+}]_i$ increase. These

findings are consistent with the effect of *p*-MCA on insulin secretion in the presence of diazoxide in INS-1 cells.

5. Enhancement of glucose-stimulated insulin release and $[Ca^{2+}]_i$ increase by *p*-MCA

The experiments were further determined the interaction between *p*-MCA and glucose on insulin secretion and $[Ca^{2+}]_i$ in INS-1 cells. Increasing glucose concentration from 5.5 mM to 10 mM caused a rapid and marked increase in insulin secretion from perfused rat pancreata (Fig 8). The first transient phase secretion peak was about 5-fold of the baseline level, which was followed a second phase that was observed after 10 min administration *p*-MCA (10 μ M) alone caused a small increase in insulin secretion, and potentiated glucose-induced insulin secretion, when added to perfusion medium 20 min after the start of glucose administration. By expressing the data as percentage of control in AUC during 20-min treatments, there was a significant difference between glucose + *p*-MCA group and glucose alone group (glucose alone = $559.1 \pm 18.0\%$; glucose + *p*-MCA = $750.3 \pm 49.3\%$). When comparing those treatments with *p*-MCA alone and control groups (control = 100.0% ; *p*-MCA 10 μ M = $129.4 \pm 8.8\%$), *p*-MCA markedly enhanced glucose-induced insulin secretion.

The effect of of *p*-MCA on glucose-induced insulin secretion was next performed in INS-1 cells using static incubation (Fig 9a and 9b). In these cells, 10 mM glucose increased insulin concentration by 65% over the control group that had 4 mM glucose. Both 10 and 100 μ M of *p*-MCA enhanced glucose-stimulated insulin secretions from INS-1 cells, which were consistent with the results in the pancreatic perfusion experiments.

$[Ca^{2+}]_i$ responses to glucose were further investigated in INS-1 cells. A rise in glucose concentrations (Fig 10) from 4 to 10 mM increased $[Ca^{2+}]_i$ in a small transient peak (120 ± 4 nM). Addition of *p*-MCA in the continued presence of glucose further potentiated the increase in $[Ca^{2+}]_i$, (10 μ M *p*-MCA = 147 ± 4 nM; 100 μ M *p*-MCA, 174 ± 5 nM).

6. Interaction between *p*-MCA and others secretagogues on insulin secretion and $[Ca^{2+}]_i$ response

The experiments were examined the effect of *p*-MCA on insulin secretion stimulated by various secretagogues, which were through different mechanisms to cause ultimate opening of the L-type Ca^{2+} channels, e.g., glyburide, which blocks K_{ATP} channels; KCl, which is a membrane depolarizing agent; Bay K 8644, which directly activates the L-type Ca^{2+} channels. Figure 11 shows the effect of *p*-MCA on insulin secretion in INS-1 cells stimulated by glyburide. Glyburide (10 μ M) significantly increased insulin secretion by 80% over the control group. The results revealed that *p*-MCA at 100 μ M, but not 10 μ M, markedly enhanced the glyburide-induced insulin secretion. The effect of glyburide on $[Ca^{2+}]_i$ response is shown in Fig. 12. When the cells was first stimulated with glyburide, the $[Ca^{2+}]_i$ response was 178 ± 8 nM (an initial peak) and being followed by a more sustained phase (133 ± 12 nM), the subsequent addition of *p*-MCA further increased $[Ca^{2+}]_i$ (10 μ M *p*-MCA = 170 ± 10 nM; 100 μ M *p*-MCA = 245 ± 18 nM).

The next experiments were investigated the effect of *p*-MCA on insulin secretion and $[Ca^{2+}]_i$ response in the presence of either of 2 secretagogues, KCl and Bay K 8644. As shown in Fig 13, KCl (15 mM) caused 3.6-fold increase in insulin secretion over the basal levels, whereas *p*-MCA (10 and 100 μ M *p*-MCA) significantly potentiated insulin secretion by 4.8- and 5.6-fold in presence the of KCl, respectively. In $[Ca^{2+}]_i$ experiments, KCl (15 mM) evoked a transient Ca^{2+} increase, which reached the peak (250 ± 10 nM) within 10 s, and followed by the sustained phase (148 ± 12 nM). Addition of *p*-MCA potentiated KCl-induced increase in $[Ca^{2+}]_i$ (Fig 14). The mean amplitude of $[Ca^{2+}]_i$ response to 10 and 100 μ M *p*-MCA were 212 ± 5 nM and 228 ± 9 nM, respectively.

The effect of *p*-MCA on Bay K 8644-stimulated insulin secretion was determined using static incubation in INS-1 cells and the pancreatic perfusion. Bay K 8644 (1 μ M) increased insulin secretion in INS-1 cells by 4-fold over the basal level (Fig 15). 10 μ M *p*-MCA and 100 μ M *p*-MCA in the presence of Bay K 8644 potentiated insulin secretion by causing 5.4- and 8.0-fold increase, respectively. This potentiation

was confirmed by experiments in the perfused rat pancreata (Fig 16). Bay K 8644 (1 μM) increased insulin secretion from the perfused rat pancreata to 2.5 times of the basal control group. The potentiation by *p*-MCA of Bay K 8644-induced insulin secretion was also observed during 30-min administration. By expressing the data as the percentage of control in AUC for Bay K 8644 and *p*-MCA as well as comparing them with those of Bay K 8644 alone, there was a significant increase in insulin secretion (control = 100 %; 10 μM *p*-MCA = $142.4 \pm 22.1\%$; Bay K 8644 = $251.2 \pm 16.6\%$; Bay K 8644 + *p*-MCA = $628.5 \pm 23.7\%$). The effects of Bay K 8644 on $[\text{Ca}^{2+}]_i$ response were also examined in INS-1 cells (Fig. 17). When Bay K 8644 (1 μM) was applied to INS-1 cells, it caused rapid and persistent increase in $[\text{Ca}^{2+}]_i$ from $89 \pm 4 \text{ nM}$ to $129 \pm 6 \text{ nM}$. *p*-MCA potentiated Bay K 8644-induced increase in $[\text{Ca}^{2+}]_i$ (10 μM *p*-MCA = $189 \pm 12 \text{ nM}$; 100 μM *p*-MCA = $225 \pm 9 \text{ nM}$).

7. Effects of *p*-MCA insulin secretion and cAMP contents in the presence of forskolin and IBMX in INS-1 cells

Since an increase in cyclic AMP content may mediate the effect of some of the insulin secretagogues, the experiments were determined if *p*-MCA increases the level of this signal in INS-1 cells. As shown in Table 1, 100 μM *p*-MCA, but not 10 μM *p*-MCA, increased cyclic AMP content by 46% in INS-1 cells. The interactions of *p*-MCA with an adenylyl cyclase activator forskolin and a phosphodiesterase inhibitor IBMX were studied as well. Forskolin (1 μM) and IBMX (100 μM) also increased cyclic AMP content. *p*-MCA (100 μM) enhanced forskolin-induced, but not IBMX-induced, increase in cyclic AMP contents. The further experiments were investigated the effects of forskolin and IBMX on *p*-MCA-induced increase in insulin secretion. The results of these experiments are shown in Fig 18 and 19. Forskolin and IBMX increased insulin secretion by 70% and 50%, respectively. *p*-MCA enhanced forskolin-induced insulin secretion (Fig. 18). In contrast, *p*-MCA failed to enhance IBMX-induced insulin secretion (Fig 19).

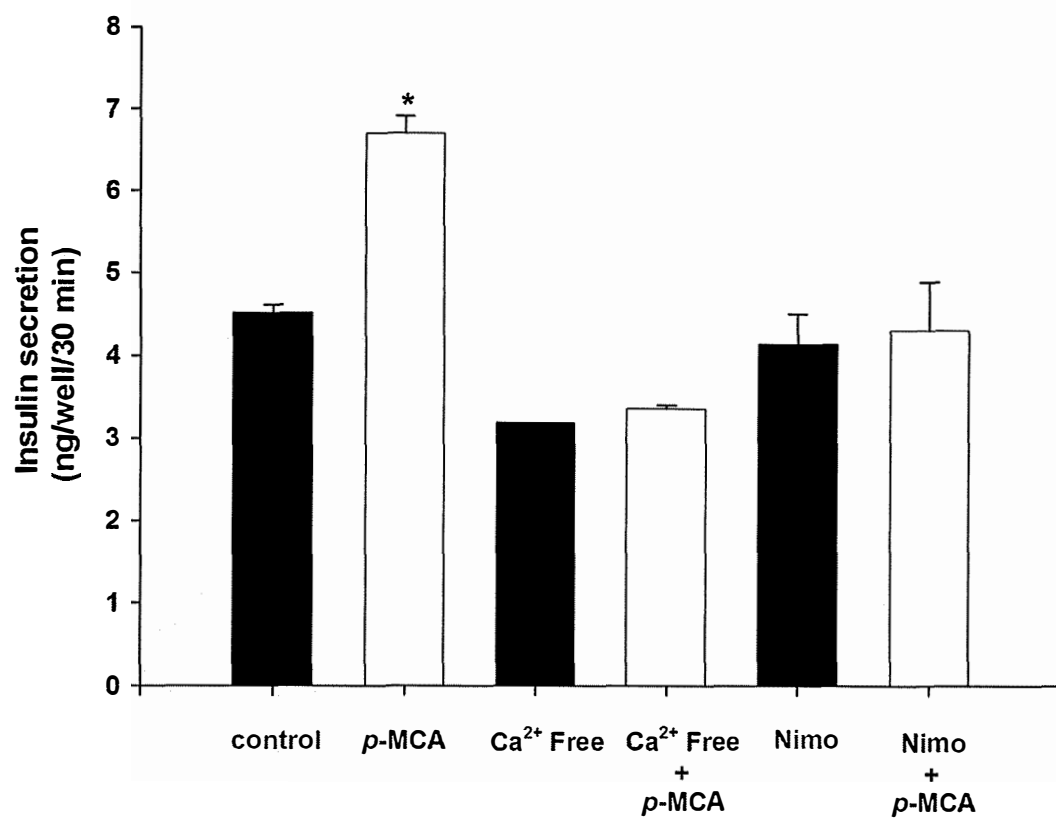


Figure 4 Effect of 100 μ M *p*-MCA on insulin secretion in INS-1 cells in the presence of Ca^{2+} free KRB or 1 μ M nimodipine(Nimo). Values are mean \pm SE; $n = 3$ independent experiments with quadruplicates in each experiment. * $P < 0.05$ compared with control.

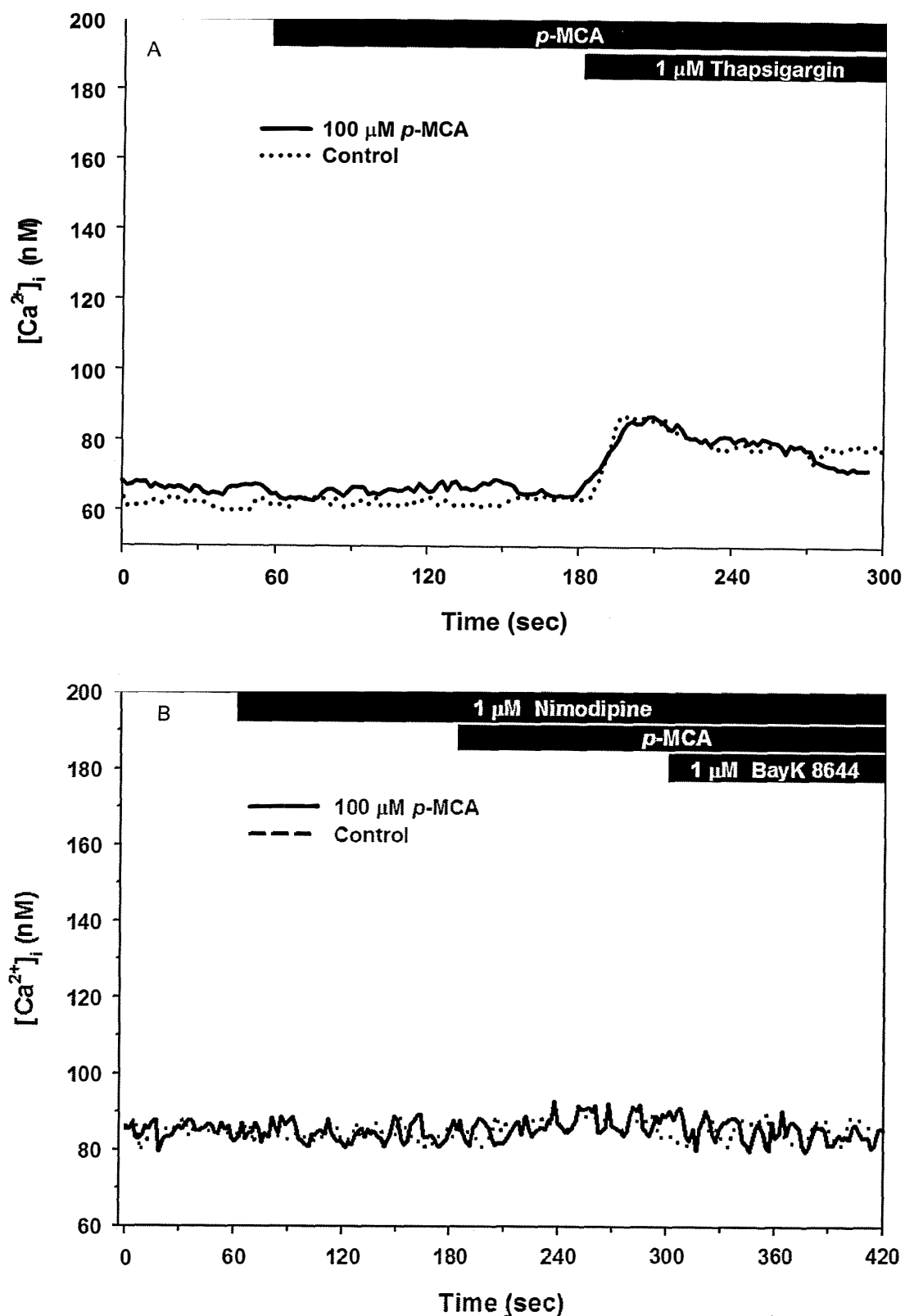


Figure 5 (A) Effect of 100 μ M *p*-MCA on $[Ca^{2+}]_i$ in the presence of Ca^{2+} free KRB. (B) Effect of 1 μ M nimodipine on 100 μ M *p*-MCA-induced increase in $[Ca^{2+}]_i$. Traces shown are representative of 4 independent experiments with 20 cells/experiment.

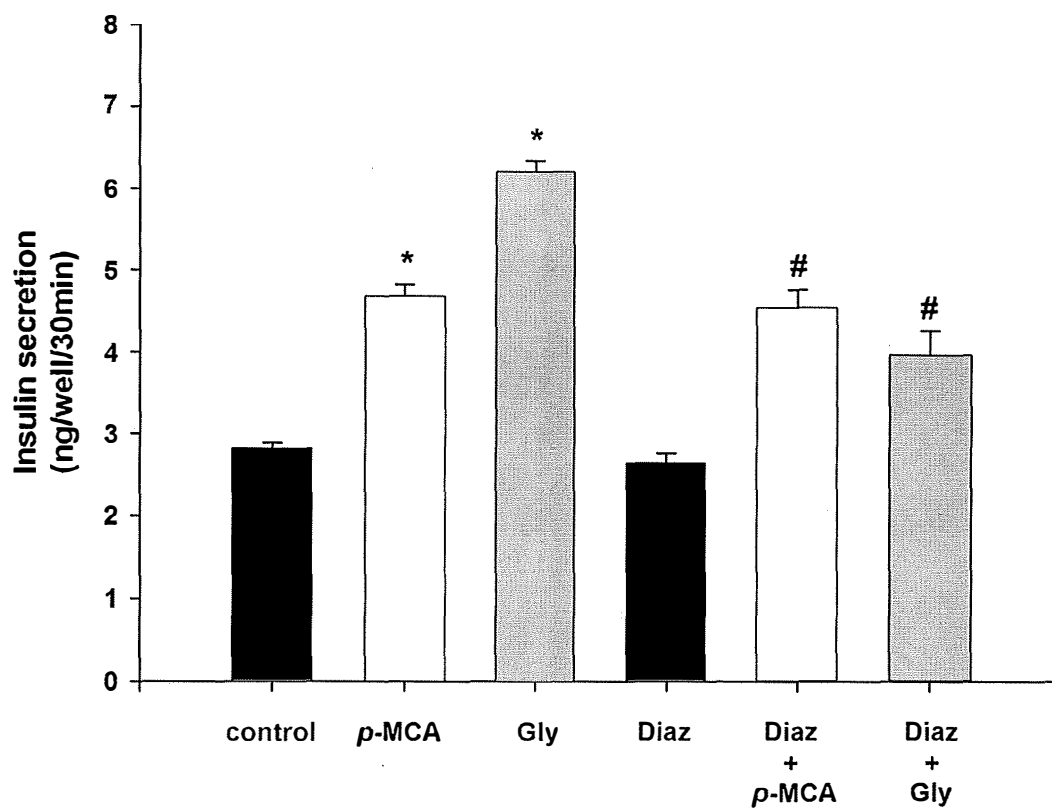


Figure 6 Effects of 400 μ M diazoxide (Diaz) on *p*-MCA (100 μ M)- and 10 μ M glyburide (Gly)-stimulated insulin secretion in INS-1 cells. Values are means \pm S.E.M.; $n = 3$ independent experiments with quadruplicates in each experiment. * $P < 0.05$ compared with control, # $P < 0.05$ compared with diazoxide alone.

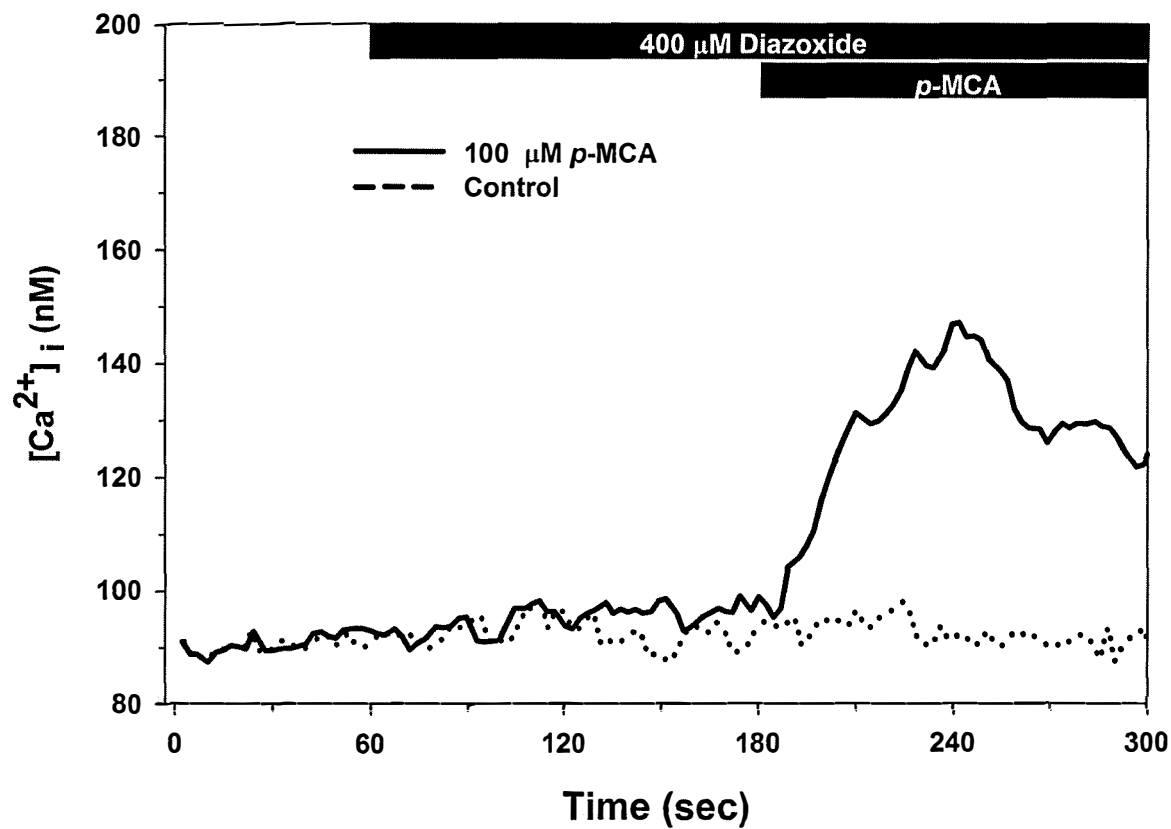


Figure 7 Effect of diazoxide on *p*-MCA-induced increase in $[Ca^{2+}]_i$. Data shown are representative of 4 independent experiments with 20 cells/experiment.

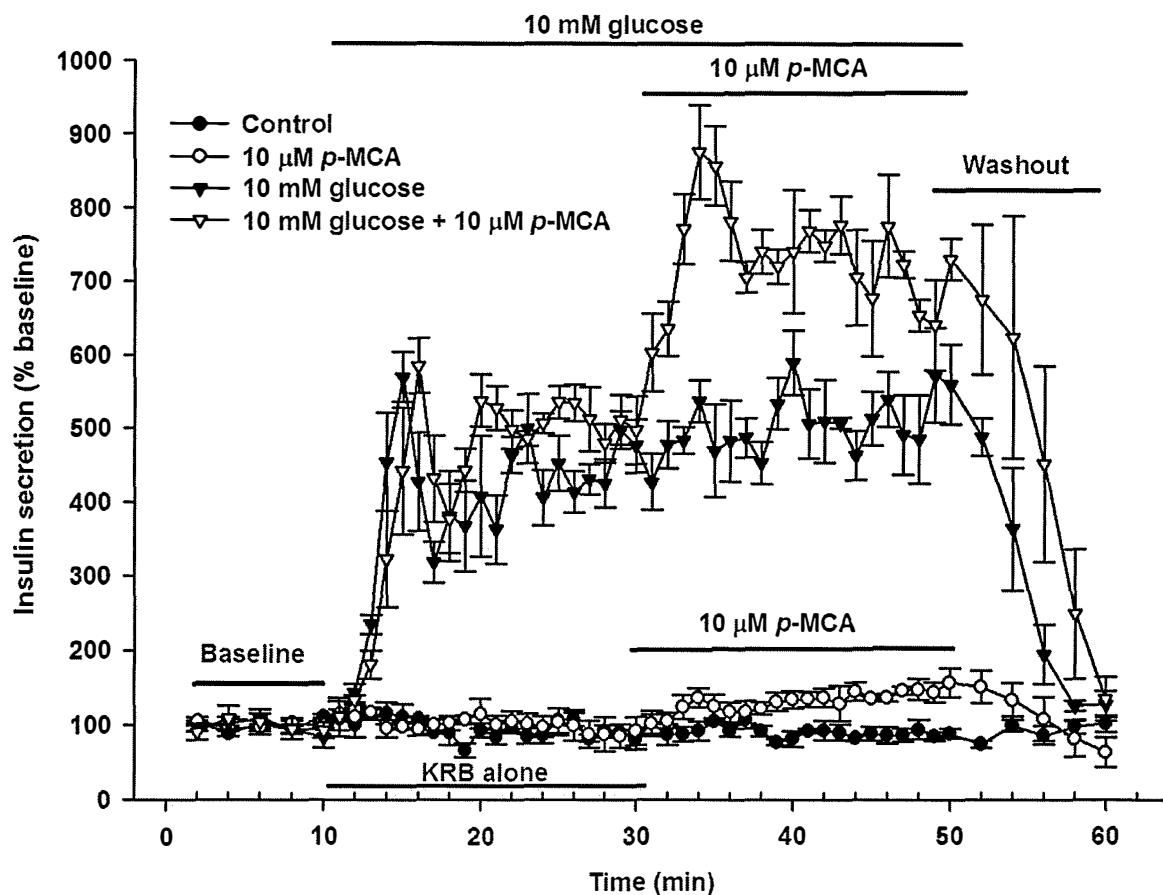


Figure 8 Effect of *p*-MCA (10 μ M) on glucose-induced insulin secretion in perfused rat pancreata. In these experiments, a 20-min equilibration period preceded *time 0*. The pancreata were perfused with KRB for a 10-min baseline period and then followed by 10 mM glucose for 20min. *p*-MCA was administered for 20 min in the presence of 10 mM glucose. Range of baseline insulin concentrations of effluents was 1.5 – 3.2 ng/ml. Values are means \pm S.E.M.; $n = 3$ pancreata.

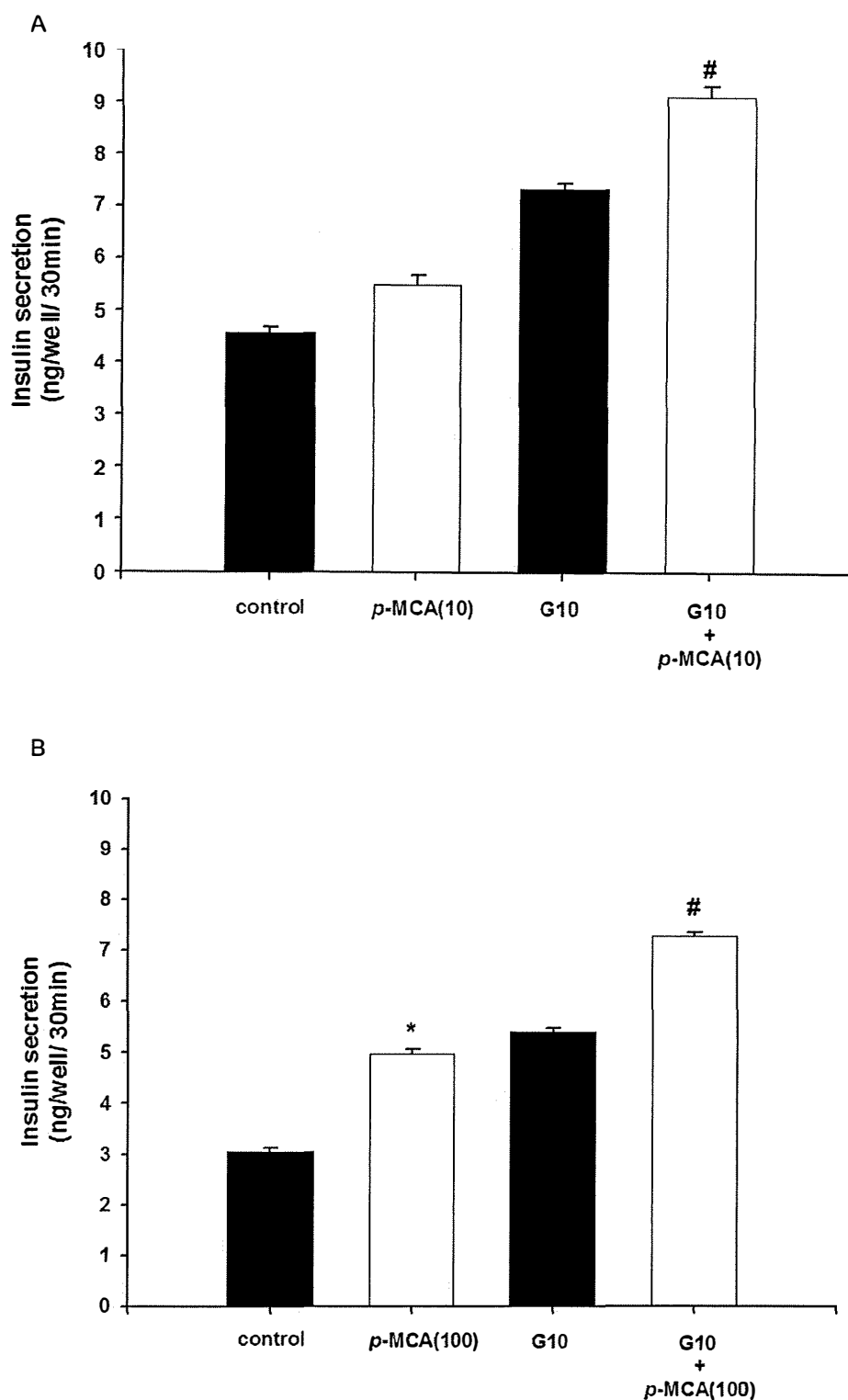


Figure 9 (A) Effect of 10 μ M *p*-MCA on glucose-induced insulin secretion in INS-1 cells. (B) Effect of 100 μ M *p*-MCA on glucose-induced insulin secretion in INS-1 cells. Values are means \pm S.E.M.; $n = 3$ independent experiments with quadruplicates in each experiment. * $P < 0.05$ compared with control (4 mM glucose alone), # $P < 0.05$ compared with 10 mM glucose alone.

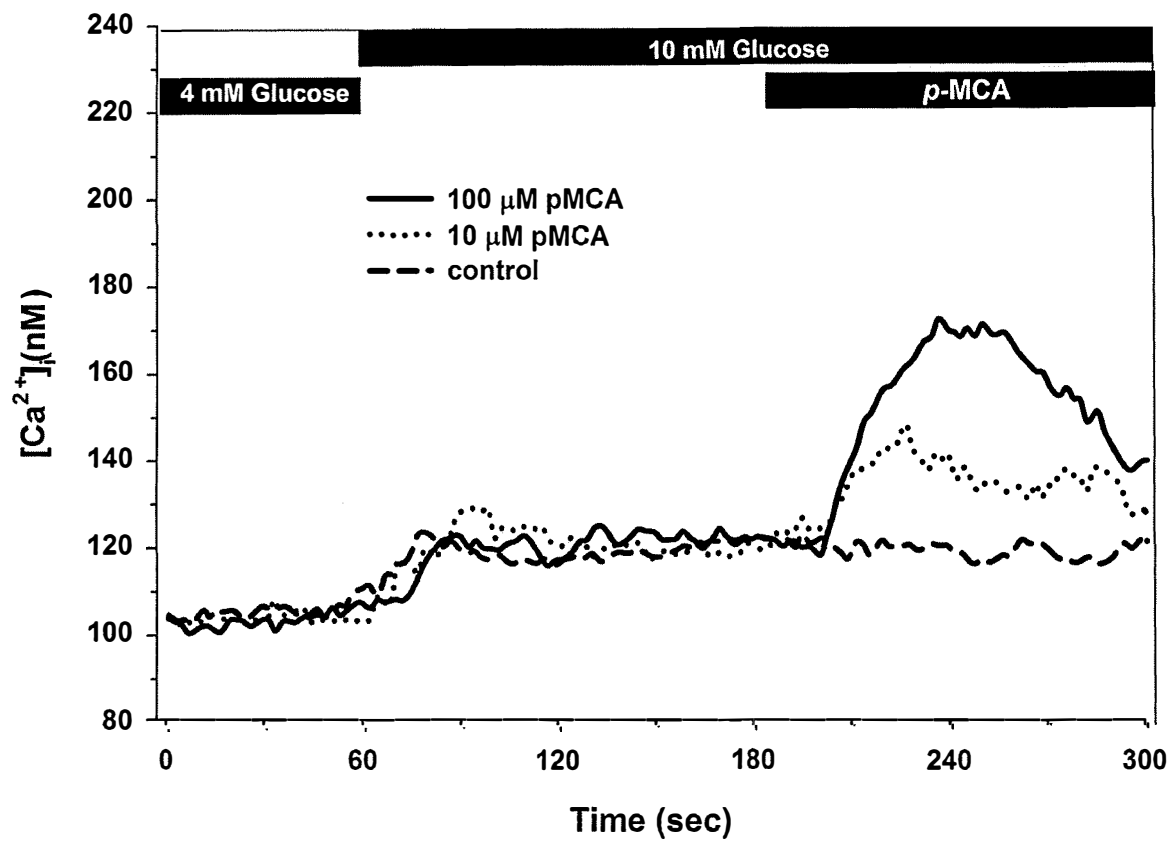


Figure 10 Effect of *p*-MCA on glucose-induced increase in $[Ca^{2+}]_i$. Data shown are representative of 4 independent experiments with 20 cells/experiment.

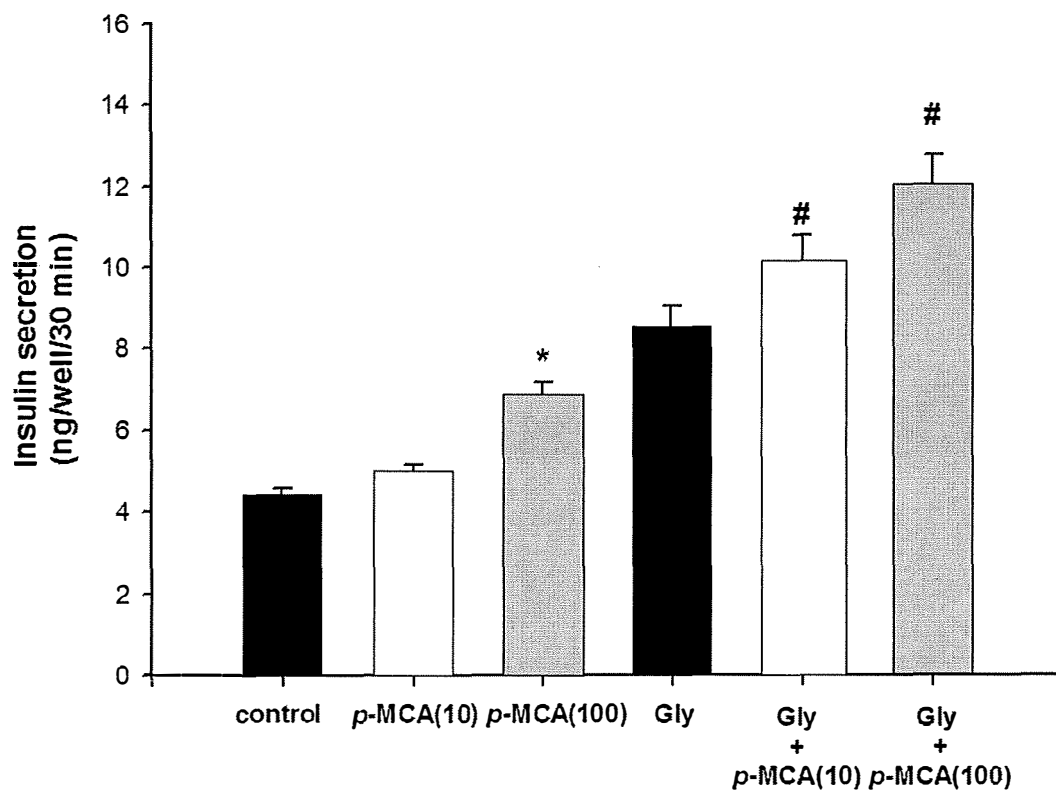


Figure 11 Effect of *p*-MCA on insulin secretion in INS-1 cells in presence of 100 μ M glyburide. Values are means \pm S.E.M.; $n = 3$ (quadruplicate) independent experiments with quadruplicates in each experiment. * $P < 0.05$ compared with control, # $P < 0.05$ compared with glyburide alone.

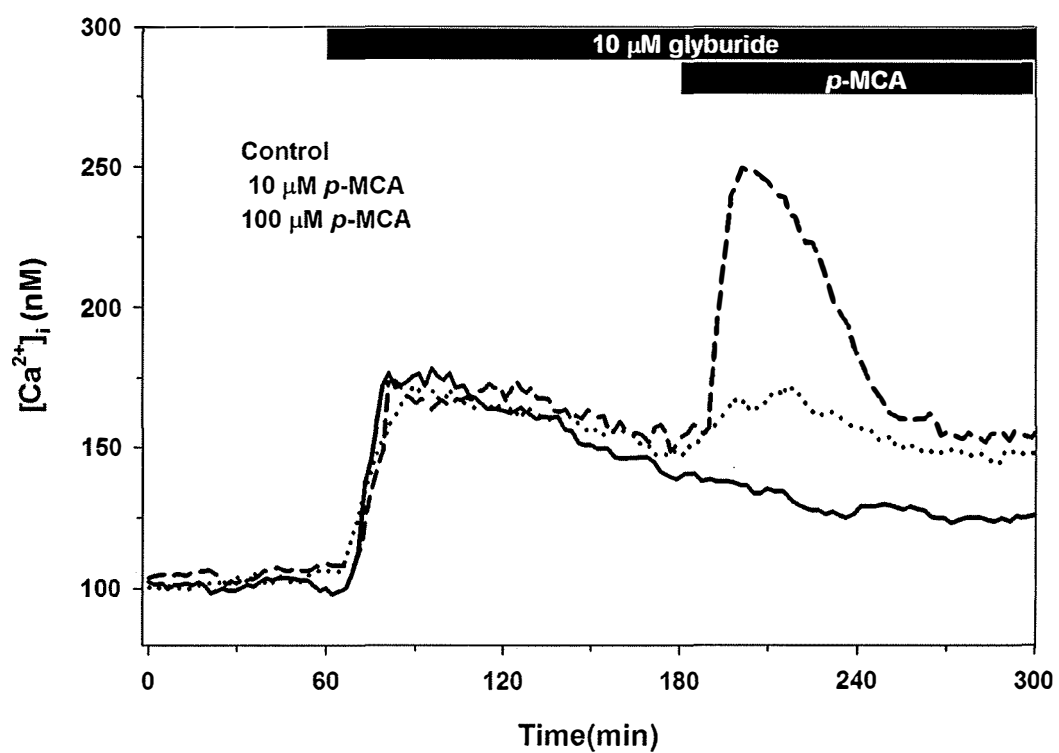


Figure 12 Effect of p-MCA on glyburide-induced $[Ca^{2+}]_i$ increase. Data shown are representative of 4 independent experiments with 20 cells/experiment.

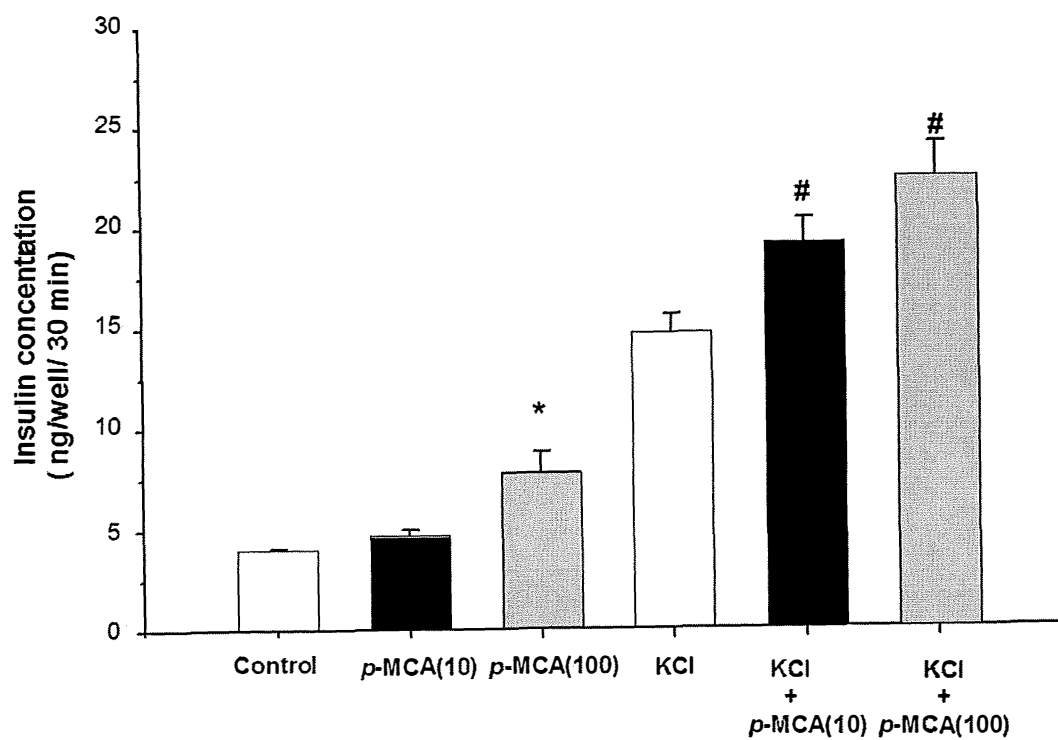


Figure 13 Effect of *p*-MCA on insulin secretion in INS-1 cells in presence of 15 mM KCl. Values are means \pm S.E.M.; $n = 3$ (quadruplicate) independent experiments with quadruplicates in each experiment. * $P < 0.05$ compared with control, # $P < 0.05$ compared with KCl alone.

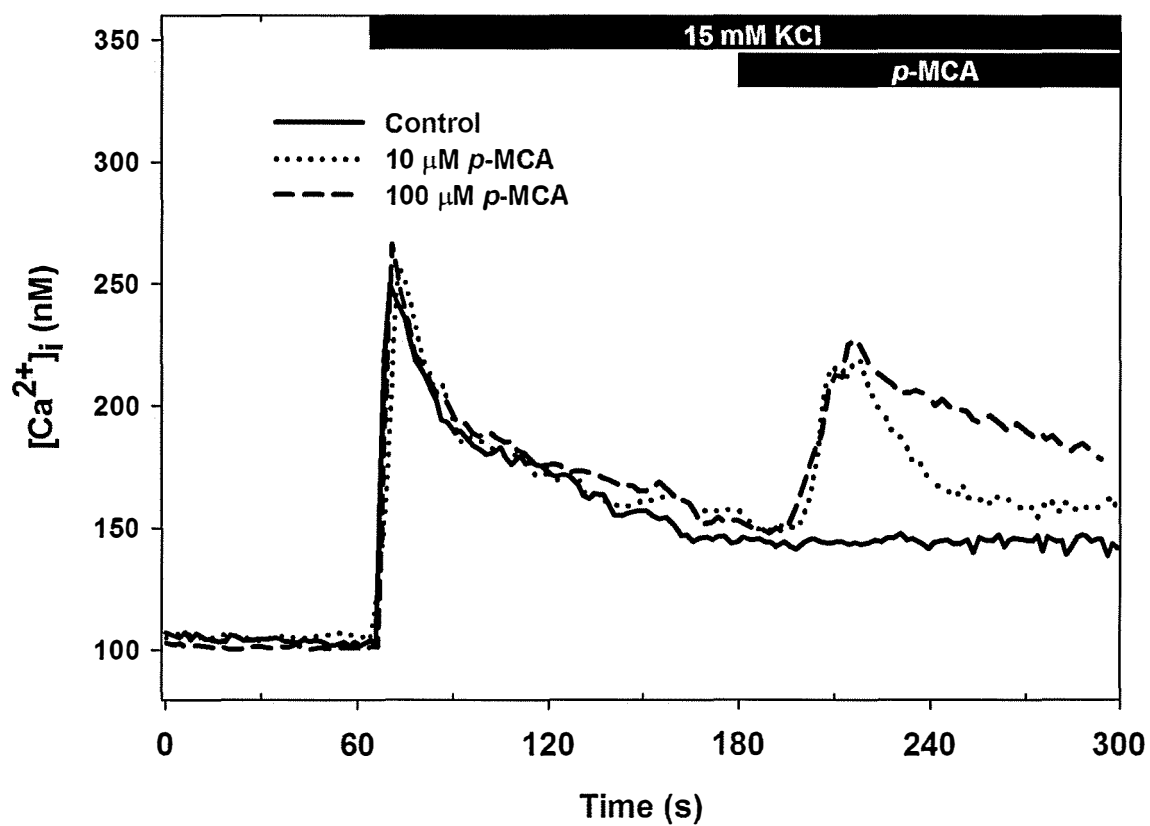


Figure 14 Effect of *p*-MCA on KCl-induced $[Ca^{2+}]_i$ increase. Data shown are representative of 4 independent experiments with 20 cells/experiment.

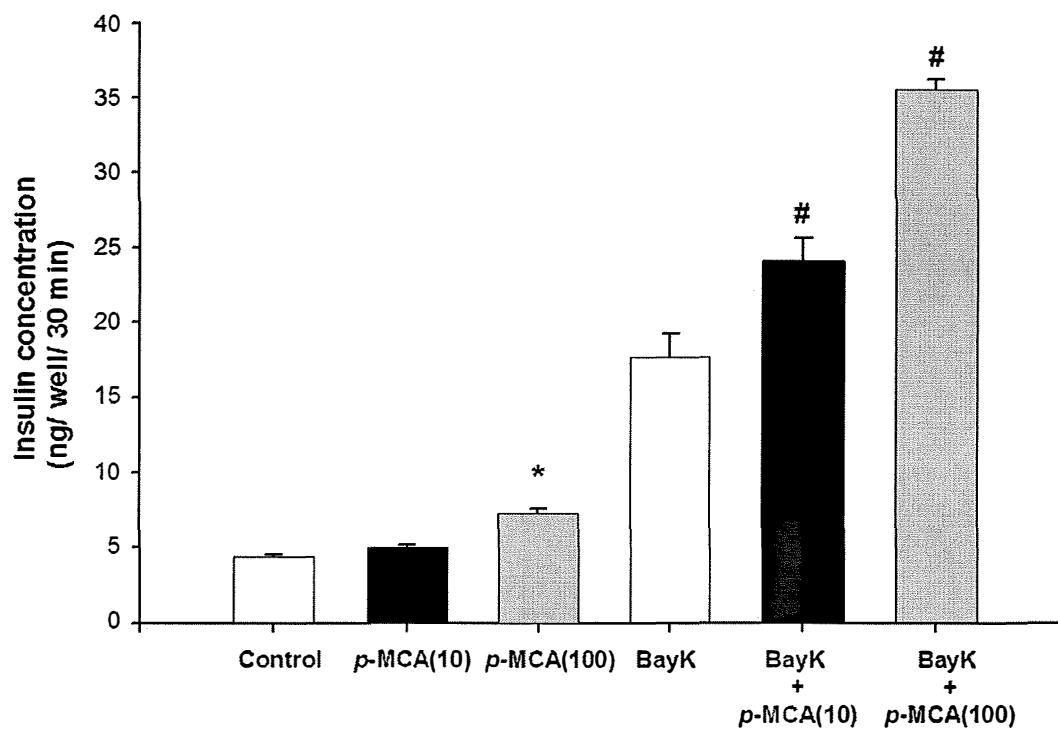


Figure 15 Effect of *p*-MCA on insulin secretion in INS-1 cells in the presence of 1 μ M Bay K 8644. Values are means \pm S.E.M.; $n = 3$ independent experiments with quadruplicates in each experiment. * $P < 0.05$ compared with control, # $P < 0.05$ compared with Bay K 8644 alone.

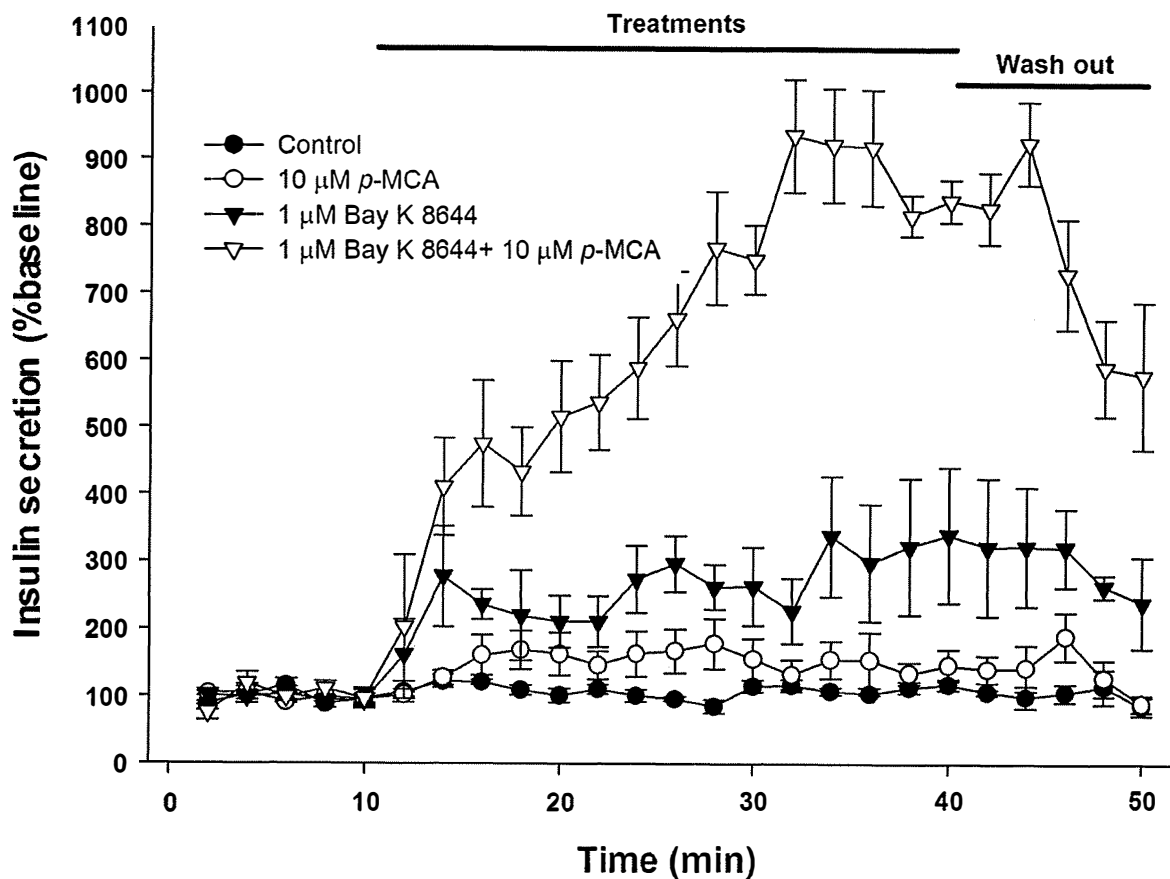


Figure 16 Effect of 10 μM p-MCA on insulin release from perfused rat pancreas. In these experiments, a 20-min equilibration period preceded *time 0*. Bay K 8644 (1 μM) was administered for 30 min with or without 10 μM p-MCA. Values are means \pm S.E.M.; $n = 3$. Range of baseline insulin concentrations of effluents was 2.2 – 3.7 ng/ml.

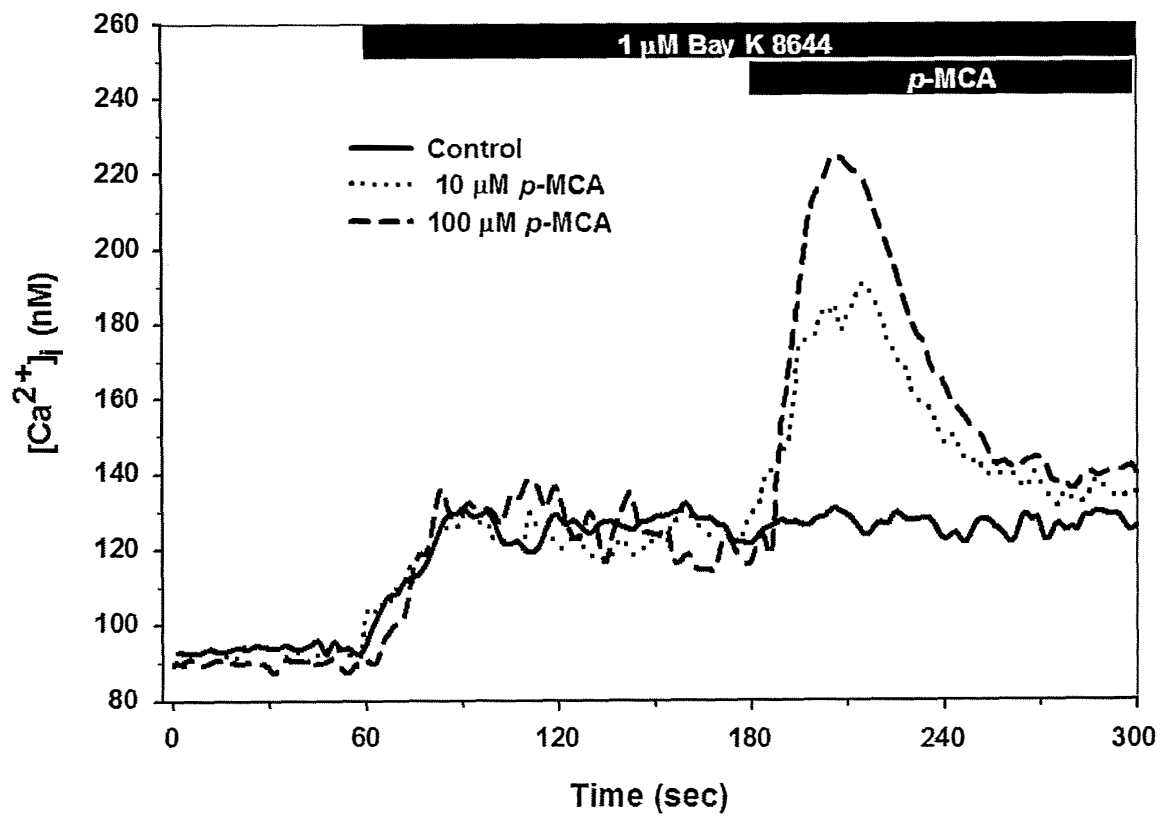


Figure 17 Effect of *p*-MCA on Bay K 8644- induced $[Ca^{2+}]_i$ response. Data shown are representative of 4 independent experiments with 20 cells/experiment.

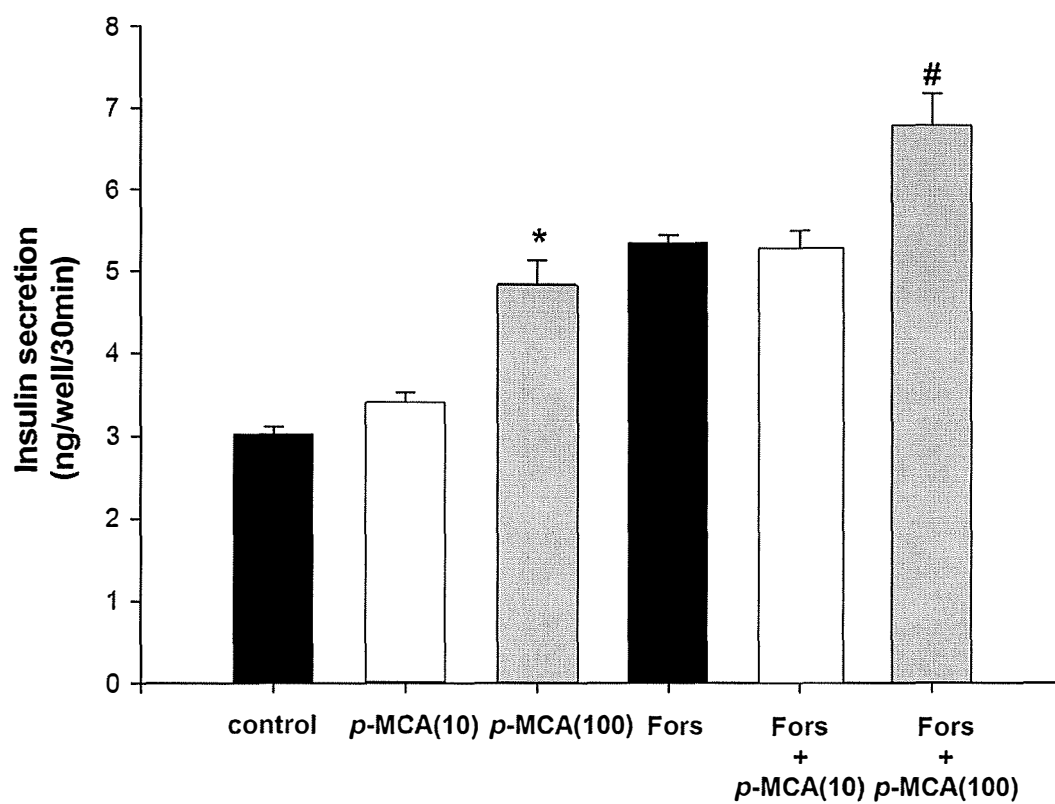


Figure 18 Effect of *p*-MCA on insulin secretion in INS-1 cells in the presence of 1 μ M forskolin(fors). Values are means \pm S.E.M.; $n = 3$ independent experiments with quadruplicates. * $P < 0.05$ compared with control, # $P < 0.05$ compared with forskolin alone.

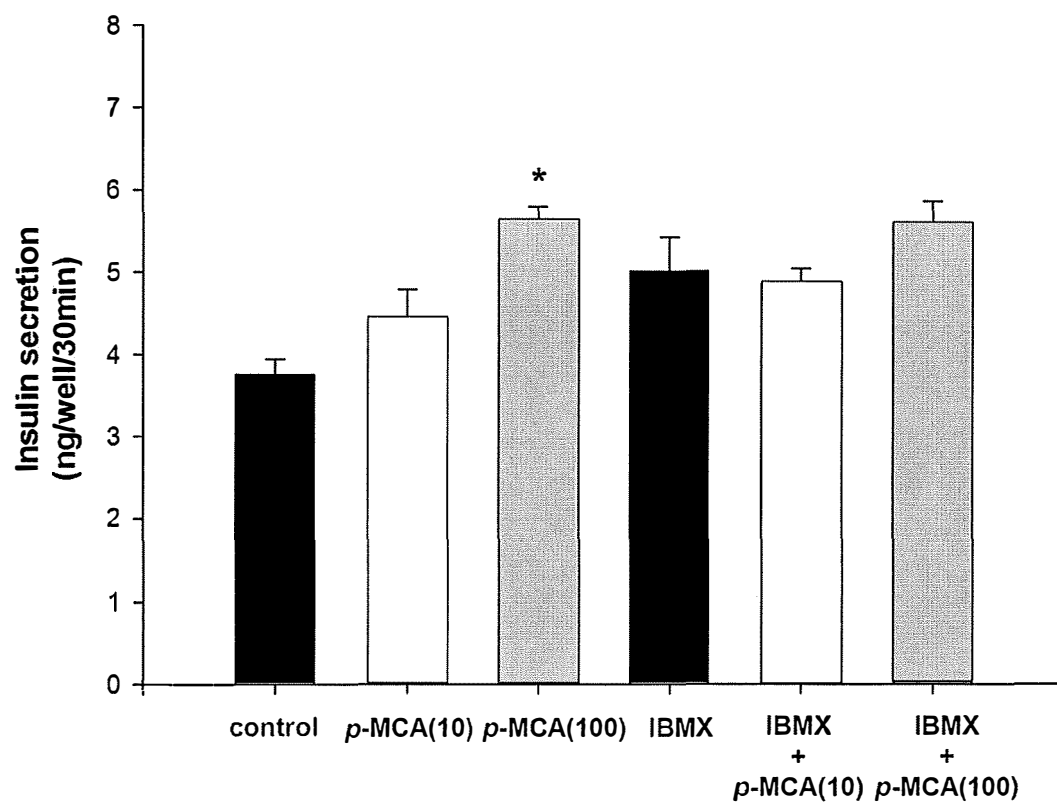


Figure 19 Effect of *p*-MCA on insulin secretion in INS-1 cells in the presence of 100 μ M IBMX. Values are means \pm S.E.M.; $n = 3$ independent experiments with quadruplicates.

* $P < 0.05$ compared with control.

Table 1 Effects of *p*-MCA on cAMP concentrations in INS-1 cells in the presence of 1 μ M forskolin and 100 μ M IBMX

cAMP level (pmol/well/ 30min)		Control	<i>p</i> -MCA(10)	<i>p</i> -MCA(100)	Forskolin	Forskolin + <i>p</i> -MCA(10)	Forskolin + <i>p</i> -MCA(10)
		1.27 \pm 0.11	1.37 \pm 0.19	1.87 \pm 0.14*	26.00 \pm 0.28	29.13 \pm 1.96	30.27 \pm 0.28 [#]
cAMP level (pmol/well/ 30min)		Control	<i>p</i> -MCA(10)	<i>p</i> -MCA(100)	IBMX	IBMX + <i>p</i> -MCA(10)	IBMX + <i>p</i> -MCA(100)
		1.08 \pm 0.32	1.21 \pm 0.04	1.76 \pm 0.14*	8.52 \pm 1.53	7.13 \pm 0.81	8.68 \pm 1.25

Values are means \pm S.E.M.; 3 independent experiments with quadruplicates in each experiment. * $P < 0.05$ compared with control, [#] $P < 0.05$ compared with forskolin alone.

8. Effect of *p*-MCA on α -glucosidases and α -amylase inhibition

Effect of *p*-MCA on α -glucosidases and α -amylase inhibition was shown in Table 2. *p*-MCA showed had more potent yeast α -glucosidase inhibiting activity ($IC_{50} = 0.04 \pm 0.01$ mM) than that of 1-deoxynorjirimycin ($IC_{50} = 5.60 \pm 0.42$ mM). However, *p*-MCA had no the inhibitory effect on mammalian α -glucosidase such as sucrase and maltase. Lineweaver-burk plot of α -glucosidase kinetics was shown in Figure 20. The kinetic result demonstrated that the mechanism of α -glucosidase inhibition of *p*-MCA was a non-competitive inhibition with K_i value of 0.060 ± 0.01 mM. Moreover, *p*-MCA had no inhibitory activity against pancreatic α -amylase.

Table 2 *In vitro* studies of inhibitory effect of *p*-MCA on α -glucosidase, and α -amylase inhibition

	Types of enzyme inhibition (IC ₅₀)			
	Yeast α -glucosidase (mM)	Mammalian α -glucosidases		Pancreatic α -amylase (μ M)
		Maltase (μ M)	Sucrase (μ M)	
<i>p</i> -MCA	0.04 \pm 0.01	N.I.	N.I.	N.I.
1-Deoxynojirimycin	5.60 \pm 0.42	N.D.	N.D.	N.D.
Acarbose	N.D.	2.51 \pm 0.37	21.82 \pm 3.23	19.80 \pm 0.15

The IC₅₀ values was expressed as means \pm S.E.M., (n=3). N.I = No inhibition, N.D. = No detection

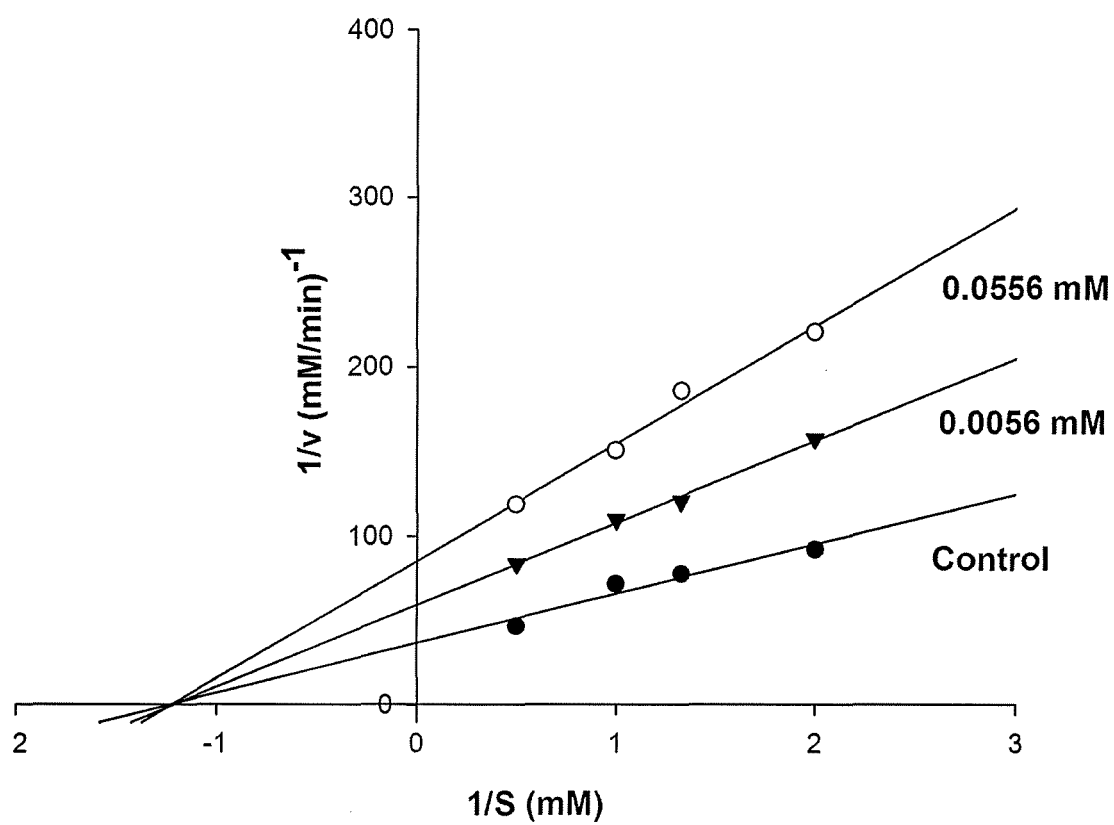


Figure 20 Lineweaver-burk plot analysis of the inhibition kinetics of α -glucosidase inhibitory effects by *p*-MCA

8. Acute toxicity of *p*-MCA in mice

In acute toxicity study, *p*-MCA (100-2000 mg/kg) caused neither visible signs of toxicity nor mortality. Generally, the reduction in body weight gain and internal organ weights is a simple and sensitive index of toxicity after exposure to toxic substance. In the present study, *p*-MCA did not produce any statistically significant difference among these three groups in both parameters. In mice treated with *p*-MCA, aspartate aminotransferase (AST), alanine aminotransferase (ALT), blood urea nitrogen (BUN), serum creatinine, cholesterol, triglycerides, HDL and LDL were not significant different when compared with mice treated with sunflower oil. The status of bone marrow activity and intravascular effects were monitored by hematological examination. In addition, the number in total white blood cells (WBC), red blood cells (RBC), platelets, lymphocytes, granulocytes and monocytes were not significant different, compared between those in *p*-MCA-treated group and control group.

9. Histopathological findings of the *p*-MCA

Pathological examination of mouse tissues (liver, kidneys, lung, heart, pancreas and brain) collected at the end of the study period (14 days) grossly revealed no pathological changes in the tissues. Using histopathology, there were no significant differences among the control and the treated groups on the heart, pancreas, lung and brain tissue.

Kidneys

There was mild degree of fat accumulation in the renal tubules of the kidneys in group 2 (sunflower oil) (Fig 21). Renal tubules of the group 5 (*p*-MCA 2,000 mg) had moderate degree of swelling and glycogen degeneration, which were demonstrated by the PAS staining and some animals (2/8 mice) found the hyaline droplets in the cytoplasm of the renal tubules (Fig 22). The other group had no remarkable lesion.

Liver

There was mild degree of fatty degeneration of the liver in group 3 (*p*-MCA 100 mg) (Fig. 23) and 4 (*p*-MCA 1,000 mg) with swollen hepatocytes. Moderate diffuse panlobular

glycogen degeneration was significantly found in all of either sex (male and female) in the group 5 (Fig. 24). The glycogen and fatty degeneration were evaluated by the PAS staining.

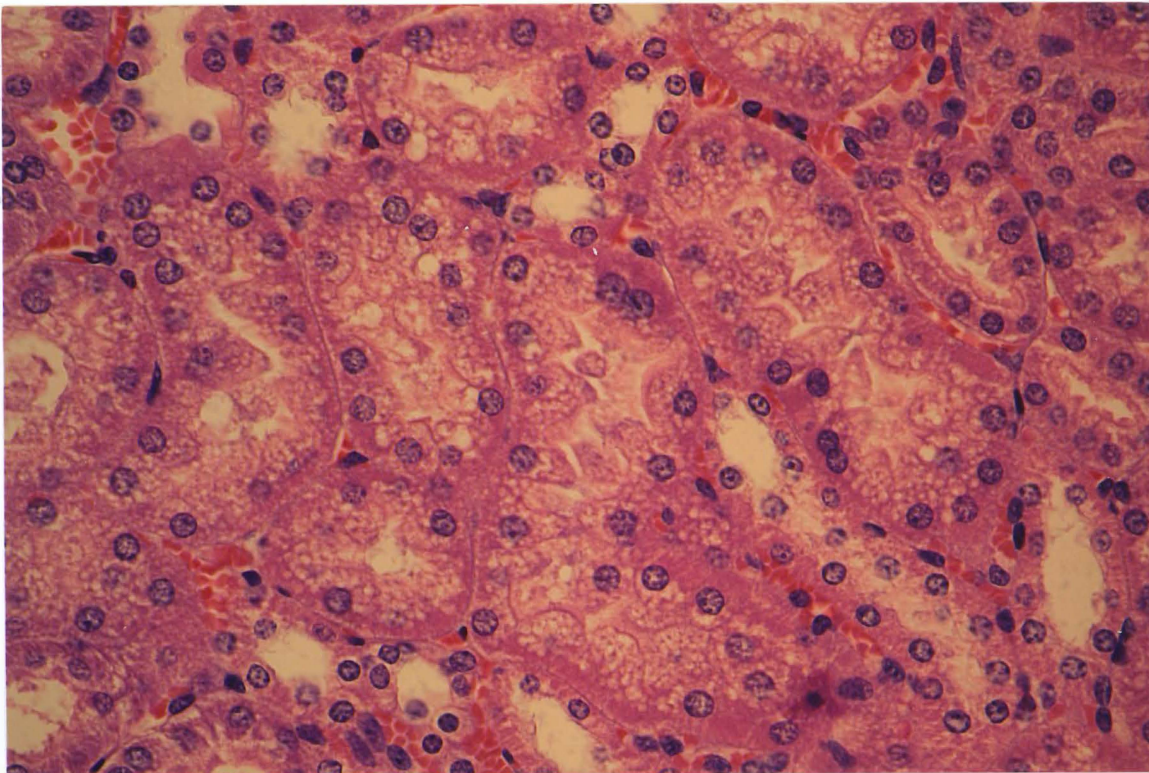


Figure 21 Mild degree of fat accumulation in the renal tubules of the kidneys in group 2.

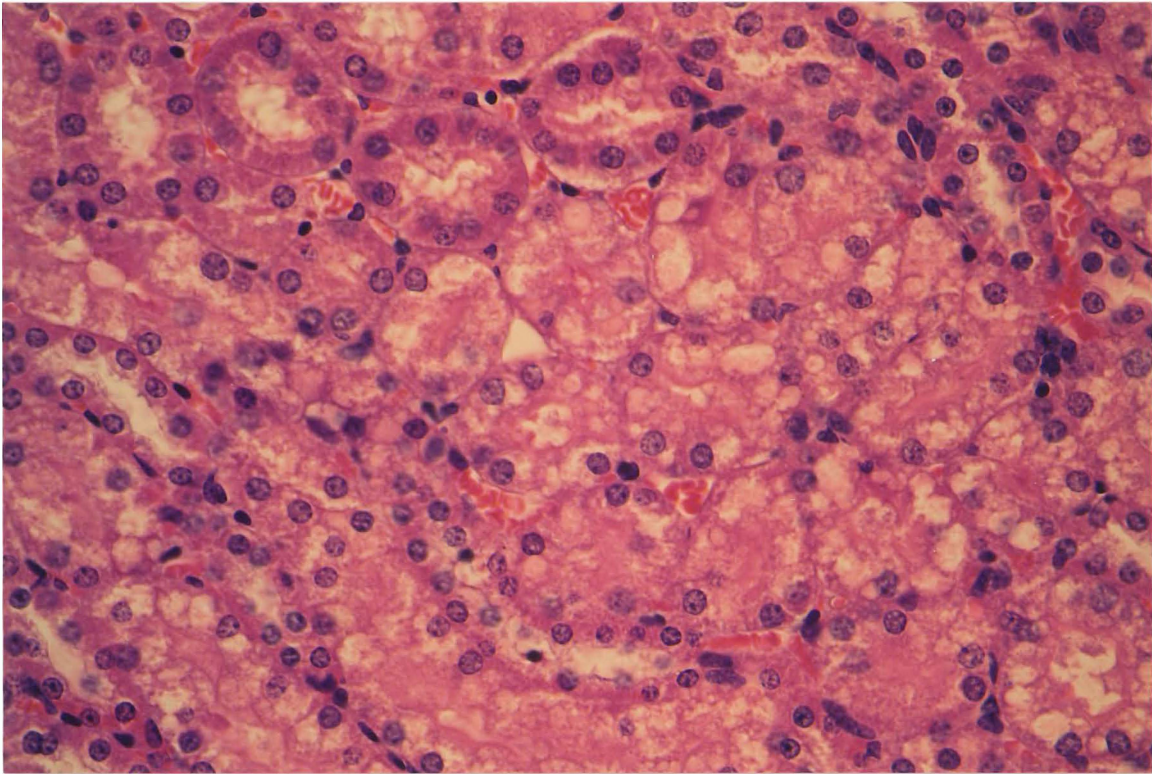


Figure 22 Moderate glycogen degeneration with the presence of hyaline droplets in the cytoplasm of the renal tubules in group 5.

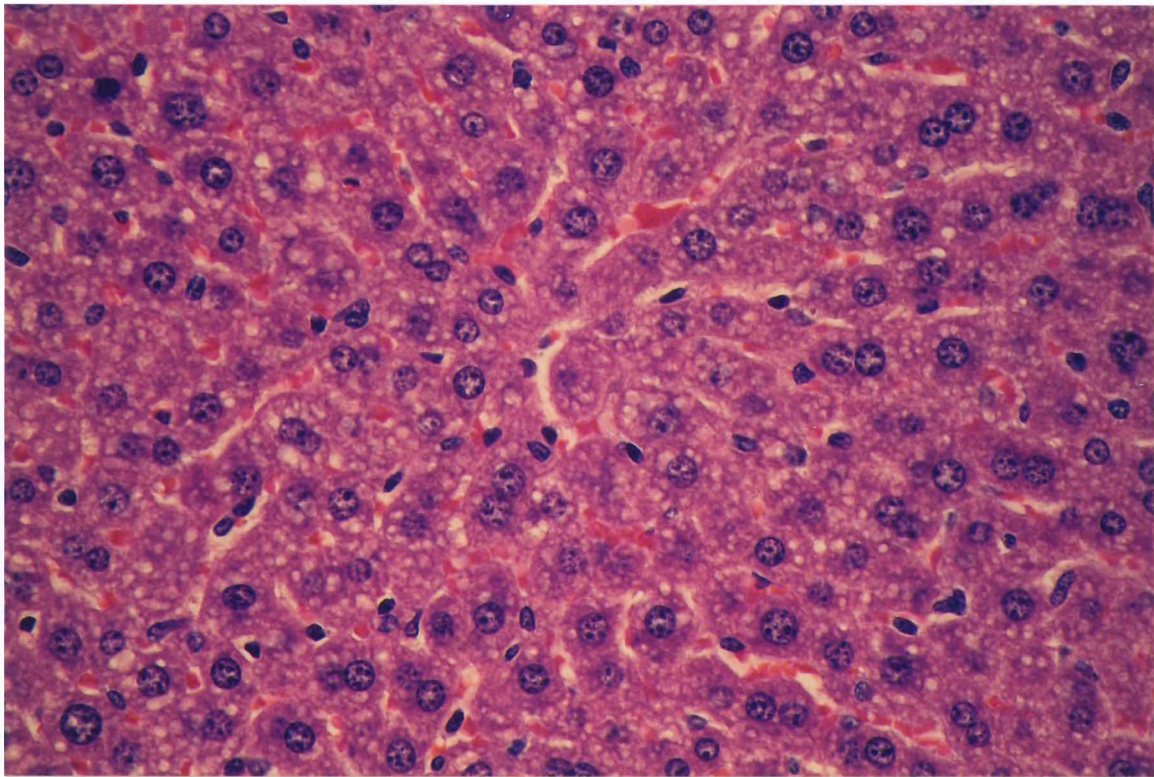


Figure 23 Mild degree of fatty degeneration in the liver of the group 3.

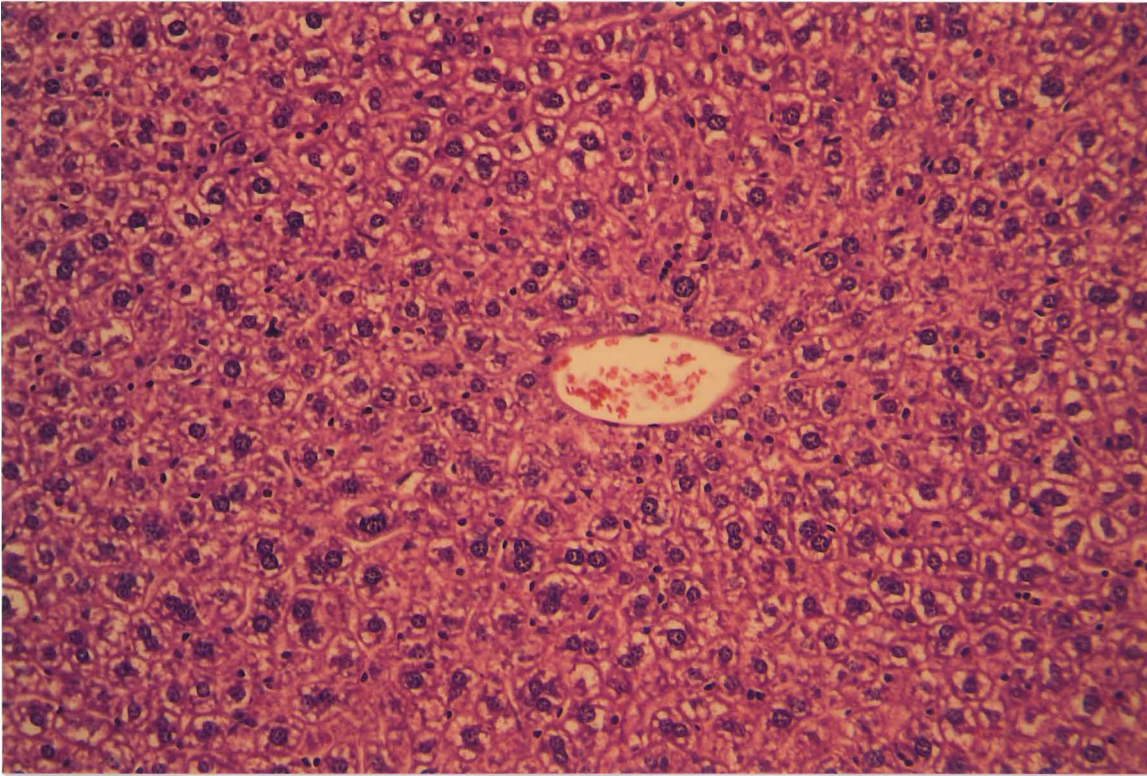


Figure 24 Moderate diffuse panlobular glycogen degeneration of the liver in the group 5.

DISCUSSION

The insulinotropic activity of *p*-MCA was determined by using the perfused rat pancreas. In agreement with the results obtained from the perfused rat pancreas, this stimulatory effect of *p*-MCA was also found in clonal β -cells INS-1, suggesting a direct effects on β -cells. The insulinoma cell line INS-1 has become a useful model for studying the molecular mechanism of Ca^{2+} -dependent and Ca^{2+} -independent insulin secretion (Wollheim, 2000). It has been shown to respond to glucose at physiological concentrations (Asfari et al., 1992). Thus, this cell line was used to study the mechanisms underlying *p*-MCA-induced insulin secretion. Moreover, the results indicated that *p*-MCA-induced $[\text{Ca}^{2+}]_i$ increase is linked to insulin secretion in INS-1 cells.

We hypothesized that *p*-MCA stimulates insulin secretion by increasing Ca^{2+} influx through L-type Ca^{2+} channels. These findings supported this hypothesis by demonstrating that the effects of *p*-MCA-induced insulin secretion were abolished under Ca^{2+} free condition and in the presence of a L- Ca^{2+} channel blocker. Such a good correlation between data obtained from insulin secretion and $[\text{Ca}^{2+}]_i$ response strongly suggests that the effects of *p*-MCA on insulin secretion from β -cells is mediated by Ca^{2+} influx through the L-type Ca^{2+} channels. The question arises as to whether the insulinotropic effect of *p*-MCA is mediated via the same mechanism as sulfonylureas. The main mechanism responsible for the insulin releasing capacity of hypoglycemic sulfonylureas implicates the closure of K_{ATP} channels, heteromultimers composed of sulfonylurea receptor (SUR) and Kir 6.2 units, leading to cell depolarization, Ca^{2+} entry and exocytosis of secretory granules (Ämmälä et al., 1996). In contrast, diazoxide behaves in the opposite manner by opening K_{ATP} channels, which leads to hyperpolarization of β -cells, thereby inhibiting insulin secretion. It is known that binding of diazoxide to its receptor partially suppresses the binding of a sulfonylurea to SUR1, and disturbs the effects of the sulfonylurea on both electrical activity and ion fluxes (Ashcroft and Ashcroft, 1992). This study showed that glyburide stimulated insulin secretion from INS-1 cells, which was partially inhibited by diazoxide. These results are consistent with previous findings

in pancreatic islets and β -cell lines (Ämmälä et al., 1996; Park et al., 2002). In contrast, diazoxide did not antagonize the stimulatory effect of *p*-MCA on insulin secretion and rise of $[Ca^{2+}]_i$, suggesting that *p*-MCA does not evoke membrane depolarization by closing of K_{ATP} channels.

Recently, cinnamic acid derivatives have been reported to exert their activities on cation channels. For examples, the transient receptor potential (TRP) family of ion channels now comprises more than 30 cation channels, most of which are permeable to Ca^{2+} (Pedersen et al., 2005). Cinnamaldehyde and cinnamic alcohol activate TRPA1 to increase Ca^{2+} influx (Bandell et al., 2004). It is well known that VDCC plays a very important role in the regulation of $[Ca^{2+}]_i$ in pancreatic β -cells. From the studies of cinnamic acid derivatives, we speculate that *p*-MCA may directly bind to L-type Ca^{2+} channels and activate them. Further study is needed to characterize the binding affinity of *p*-MCA on L-type Ca^{2+} channels and to determine the effect of *p*-MCA on these channels.

Our results showed that the direct exposure of pancreatic β -cells to *p*-MCA in the presence of glucose amplified the insulin secretion. In STZ-induced diabetic rats, *p*-MCA (40 mg/kg) decreased plasma glucose concentration and increased insulin concentration after glucose loading. Therefore, *p*-MCA improves glucose intolerance in diabetic rats. Our findings suggested that *p*-MCA may be beneficial to patients with diabetes mellitus who have defects in the response of insulin secretion to glucose stimulation.

The experiments were further investigated whether *p*-MCA potentiates the effects of other secretagogues than glucose. Glyburide is an antidiabetic agent, which has been used in those patients with maturity onset or type 2 diabetes. In this study, glyburide (10 μ M) produced the maximum effective concentration on insulin secretion in INS-1 cells (data not shown). *p*-MCA at 100 μ M exerted the additive effect of glyburide on insulin secretion. These findings suggested that *p*-MCA may benefit the use of glyburide in the control of type 2 diabetes.

The depolarization of membrane by a rise of extracellular KCl and the opening of L-type Ca^{2+} channel by Bay K 8644 could potentiate the effect of *p*-MCA-induced insulin secretion. Bay K 8644 is a dihydropyridine (DHP) compound, which increases the mean open time and opens probability of the L-type Ca^{2+} channels in a variety of cells (Striessnig et al., 1991), including cardiac cells (Skasa et al., 2001) and β -cells (Larsson-Nyren and Sehlin, 1996). L-type Ca^{2+} channels are complex proteins that consist of a pore-forming α_1 subunit, disulfide-linked transmembrane complex of α_2 and δ subunits (α_2/δ), intracellular β subunit, and γ subunit. α_1 Subunits are further divided into five major subtypes based on biophysical and pharmacological characteristics (Hofmann et al., 1999). DHP compounds bind to L-type Ca^{2+} channel α_1 subunits with high affinity. Interestingly, DHP at high concentrations or administered at depolarized membrane potentials can close these channels (Usowicz et al., 1995). Similarly, a benzoylpyrrole derivative, FPL-64176, a classical Ca^{2+} channel agonist, increase in $[\text{Ca}^{2+}]_i$ and subsequent insulin release from β TC3-cells (Springborg et al., 1997). These compounds act at the same region but bind to the different amino acid residue within III5 and III6 transmembrane segments of L-type Ca^{2+} channel α_{1c} subunit (Rampe and Lacerda, 1991; Zheng et al., 1991). Thus, we speculate that *p*-MCA potentiates Bay K 8644-induced insulin secretion by activating of the different binding site or subunit of the L-type Ca^{2+} channel. Further work is needed to prove this speculation.

Since, *p*-MCA (100 μM) enhanced forskolin-induced insulin secretion and cAMP content but it failed to increase IBMX-induced insulin secretion and cAMP content. These results suggested that the agent may increase insulin secretion and cAMP content by inhibiting PDE. Several studies have reported the presence of both PDE3 and PDE4 in pancreatic islets (Beavo, 1995), but only the inhibitors specific for PDE3 actually potentiate insulin secretion (Shafiee-Nick et al., 1995; Parker et al., 1995). It is likely *p*-MCA inhibits PDE3 to increase cAMP content in β -cells. Further studies are needed to determine which PDE isoform is inhibited by *p*-MCA in β -cells. On the other hand, the *p*-MCA (100 μM)-induced increase in cAMP level was much less than those induced IBMX (100 μM) or forskolin (1 μM). Interestingly, forskolin increased cAMP levels by ~ 20 fold, but the increase in insulin secretion was only 1.6 fold of the

basal control group. Thus, *p*-MCA-induced increase in cAMP probably plays a minor role in its insulinotropic effect.

As the results of α -glucosidase inhibition, was the potent yeast α -glucosidase inhibitor which is the competitive inhibition. Acarbose showed a potent mammalian α -glucosidase and α -amylase inhibitor, whereas *p*-MCA had no any inhibitory activity on these enzymes activity. These findings suggested that *p*-MCA has more specific inhibition on yeast than mammalian α -glucosidase.

Recent years have apparent evidence of the inhibitory α -glucosidase activities through interference with biosynthesis of glycoprotein processing on the surface of the viral cell wall, which have exhibited promising activities as anti-viral agents. *N*-linked oligosaccharides play roles in the fate and functions of glycoproteins. One function is to assist in the folding of proteins by mediating interactions of the lectin-like chaperone proteins calnexin and calreticulin with nascent of the α -glucosidases. This causes some proteins to be misfolded and retained within the endoplasmic reticulum. HIV-1, the causative agent of acquired immunodeficiency syndrome (AIDS), encodes two essential envelope glycoproteins (gp120 and gp41) through the endoproteolytic cleavage of the precursor protein within *cis*-golgi apparatus by α -glucosidases activities (Robina et al., 2004). Treatment of HIV-1 infected cells with N-butyldeoxynojirimycin (NB-DNJ), an inhibitor of the α -glucosidases, inhibits syncytium formation and the formation of infectious virus (Fischer et al., 1995). Thus, *p*-MCA may lead to be a new anti-HIV agent in the future.

The regulation of carbohydrate absorption via inhibition of these luminal α -glucosidases effectively reduces postprandial hyperglycemia, and thus, improves glycemic control in patients with type 2 diabetes mellitus. The main digestible carbohydrates in human diet are starch and sucrose. Starch granules constitute a mixture of two different plant polysaccharides, amylose, a linear $[4\text{-O-}\alpha\text{-D-glucopyranosyl-D-glucose}]_n$ polymer, and amylopectin, with additional $6\text{-O-}\alpha\text{-D-glucopyranosyl-D-glucose}$ links in the branched structure. In view of nutritional information, dietary starches are a mixture of 25% amylose with 75% amylopectin (Nichols et al., 2003). The processing of starch digestion begins in the intestinal

lumen by α -amylase, which is found in salivary and pancreatic secretions, producing linear malto-oligosaccharides and α -limit dextrins containing both α -(1 \rightarrow 4) linkages and one or more α -(1 \rightarrow 6) branching links. Both families of malto-oligosaccharides are not absorbable without further processing to glucose by hydrolysis at the nonreducing ends of 1-4 and 1-6 oligomers by α -glucosidase enzymes (Nichols et al., 1998). α -Glucosidase enzymes (sucrase, isomaltase, maltase, glycoamylase and trehalase) break down non-absorbable complex carbohydrate into absorbable monosaccharides at the brush border membrane of enterocyte in small intestine before transportation of glucose across intestinal microvilli to circulation (Bischoff, 1995). The antidiabetic drugs of the family of α -glucosidase inhibitors comprise three compounds: acarbose, which is the best studied, and most widely used agent.

Additional structure-activity relationship studies on yeast α -glucosidase inhibition, *p*-MCA showed the highest potent inhibitory activity among those of seventeen cinnamic acid derivatives. Additional studies on structure-activity relationship, the presence of substituents at *para*-position in cinnamic acid altered the α -glucosidase inhibitory activity. The increase of bulkiness and the chain length of *para*-alkoxy substituents as well as the increasing of the electron withdrawing group have been shown to decrease the inhibitory activity.

The acute toxicity of *p*-MCA (100-2000 mg/kg) was examined in mice. The result showed that *p*-MCA produced neither mortality nor significant differences in blood chemistry profiles when compared to those in the control group. Neither gross abnormalities nor histopathological changes of brain, pancreas, heart and lung were observed. However, in the liver, histopathological examinations revealed mild degree of fatty degeneration in both *p*-MCA (100 mg)- and (*p*-MCA 1,000 mg)-treated groups. In addition, moderate diffuse panlobular glycogen degeneration in liver and renal tubules were found in (*p*-MCA 2,000 mg)-treated groups. It is possible that *p*-MCA decreases the activity of glucose-6-phosphatase (Adisakwattana et al., 2005), which is a crucial enzyme for the final step of glycogenolysis, therefore, the excessive amounts of glycogen were accumulated in liver and renal tubules. Further studies in subacute and chronic toxicity tests are warranted to confirm the safety profile of *p*-MCA.

REFERENCES

- Adisakwattana S, Sookkongwaree K, Roengsumran S, Petsom A, Ngamrojnavanich N, Chavasiri W, Deesamer S, and Yibchok-anun S (2004) Structure-activity relationships of trans-cinnamic acid derivatives on alpha-glucosidase inhibition. *Bioorg Med Chem Lett* 14:2893-2896.
- Adisakwattana S, Roengsamran S, Hsu WH, and Yibchok-Anun S (2005) Mechanisms of antihyperglycemic effect of p-methoxycinnamic acid in normal and streptozotocin-induced diabetic rats. *Life Sci* 78:406-412.
- Ämmälä C, Moorhouse A, and Ashcroft FM (1996) The sulphonylurea receptor confers diazoxide sensitivity on the inwardly rectifying K⁺ channel Kir6.1 expressed in human embryonic kidney cells. *J Physiol* 494:709-714.
- Asfari M, Janjic D, Meda P, Li G, Halban PA, and Wollheim CB (1992) Establishment of 2-mercaptoethanol-dependent differentiated insulin-secreting cell lines. *Endocrinology* 130:167-178.
- Ashcroft FM (2005) ATP-sensitive potassium channelopathies: focus on insulin secretion. *J Clin Invest* 115:2047-2058.
- Ashcroft SJH and Ashcroft FM (1992) The sulfonylurea receptor. *Biochim Biophys Acta* 11:75:45-59.
- Bandell M, Story GM, Hwang SW, Viswanath V, Eid SR, Petrus MJ, Earley TJ, and Patapoutian A (2004) Noxious cold ion channel TRPA1 is activated by pungent compounds and bradykinin. *Neuron*. 41: 849-857.
- Beavo JA (1995) Cyclic nucleotide phosphodiesterases: functional implications of multiple isoforms. *Physiol Rev* 75:725-48.
- Bischoff H (1995) The mechanism of alpha-glucosidase inhibition in the management of diabetes. *Clin Invest Med* 18:303-311.
- Bylka W (2004) E- and Z-p-methoxycinnamic acid from *Aquilegia vulgaris*. *Acta Pol Pharm* 61:307-308.

- Cheng H, Grodnitzky JA, Yibchoğ-anun S, Ding J, and Hsu WH (2005) Somatostatin increases phospholipase D activity and phosphatidylinositol 4,5-bisphosphate synthesis in clonal β -cells HIT-T15. *Mol Pharmacol* 67:2162-2172.
- Ferner RE and Neil HAW (1988) Sulphonylureas and hypoglycaemia. *Br Med J* 296: 949-950.
- Fischer PB, Collin M, Karlsson GB, James W, Butters TD, Davis SJ, Gordon S, Dwek RA and Platt FM. (1995) The alpha-glucosidase inhibitor N-butyldeoxynojirimycin inhibits human immunodeficiency virus entry at the level of post-CD4 binding. *J Virol* 69:5791-5797.
- Gerich JE (1989) Oral hypoglycemic agents. *N Engl J Med* 321:1231-1245.
- Gonoi T, Mizuno N, Inagaki N, Kuromi H, Seino Y, Miyazaki J, and Seino S (1994) Functional neuronal ionotropic glutamate receptors are expressed in the non-neuronal cell line MIN6. *J Biol Chem* 269:16989-16992.
- Hofmann F, Lacinova L, and Klugbauer N (1999) Voltage-dependent calcium channels: from structure to function. *Rev Physiol Biochem Pharmacol*. 139: 33-87.
- Jackson JE and Bressler R (1981) Clinical pharmacology of sulphonylurea hypoglycaemic agents: part 1. *Drugs* 22:211-245.
- Jennings A, Wilson R, and Ward J (1989) Symptomatic hypoglycemia in NIDDM patients treated with oral hypoglycemic agents. *Diabetes Care* 12:203-208.
- Kim SR, Sung SH, Jang YP, Markelonis GJ, Oh TH, and Kim YC (2002) E-p-methoxycinnamic acid protects cultured neuronal cells against neurotoxicity induced by glutamate. *Br J Pharmacol* 135:1281-1291.
- Kim SR, Kang SY, Lee KY, Kim SH, Markelonis GJ, Oh TH, and Kim YC (2003) Anti-amnestic activity of E-p-methoxycinnamic acid from *Scrophularia buergeriana*. *Brain Res Cogn Brain Res* 17:454-461.
- Larsson-Nyren G and Sehlin J (1996) Comparison of the effects of perchlorate and Bay K 8644 on the dynamics of cytoplasmic Ca^{2+} concentration and insulin secretion in mouse beta-cells. *Biochem J* 314:67-173.
- Lee EJ, Kim SR, Kim J, and Kim YC (2002) Hepatoprotective phenylpropanoids from *Scrophularia buergeriana* roots against CCl_4 -induced toxicity: action mechanism and structure-activity relationship. *Planta Med* 68:407-411.

- Liu IM, Chi TC, Hsu FL, Chen CF and Cheng JT (1999) Isoferulic acid as active principle from the rhizoma of *Cimicifuga dahurica* to lower plasma glucose in diabetic rats. *Planta Medica* 65:712-714.
- Mayer ML and Armstrong N (2004) Structure and function of glutamate receptor ion channels. *Annu Rev Physiol* 66:161-181.
- Natella F, Nardini M, Di Felice M, and Scaccini C (1999) Benzoic and cinnamic acid derivatives as antioxidants: structure-activity relation. *J Agric Food Chem* 47:1453-1459.
- Nichols BL, Avery S, Sen P, Swallow DM, Hahn D and Sterchi E (2003) The maltase-glucoamylase gene: common ancestry to sucrase-isomaltase with complementary starch digestion activities. *Proc Natl Acad Sci U S A* 100:1432-1437.
- Nichols BL, Eldering J, Avery S, Hahn D, Quaroni A and Sterchi E (1998) Human small intestinal maltase-glucoamylase cDNA cloning. Homology to sucrase-isomaltase. *J Biol Chem* 273:3076-3081.
- Nomura E, Kashiwada A, Hosoda A, Nakamura K, Morishita H, Tsuno T, and Taniguchi H (2003) Synthesis of amide compounds of ferulic acid, and their stimulatory effects on insulin secretion in vitro. *Bioorg Med Chem* 11:3807-3813.
- Park KH, Song SC, and Akaike T (2002) Determination of the specific interaction between sulfonylurea-incorporated polymer and rat islets. *J Biochem (Tokyo)* 131:359-364.
- Parker JC, VanVolkenburg MA, Ketchum RJ, Brayman KL, and Andrews KM (1995) Cyclic AMP phosphodiesterases of human and rat islets of Langerhans: contributions of types III and IV to the modulation of insulin secretion. *Biochem Biophys Res Commun* 217:916-23.
- Pedersen SF, Owsianik G and Nilius B (2005) TRP channels: an overview. *Cell Calcium* 38: 233-252
- Perez-Alvarez V, Bobadilla RA, and Muriel P (2001) Structure-hepatoprotective activity relationship of 3,4-dihydroxycinnamic acid (caffeic acid) derivatives. *J Appl Toxicol* 21:527-531.
- Prapong T, Uemura E, and Hsu WH (2001) G protein and cAMP-dependent protein kinase mediate amyloid beta-peptide inhibition of neuronal glucose uptake. *Exp Neurol* 167:59-64.

- Rajan AS, Aguilar-Bryan L, Nelson DA, Yaney GC, Hsu WH, Kunze DL, and Boyd AE (1990) Ion channels and insulin secretion. *Diabetes Care* 13:340-363.
- Rampe D and Lacerda AE (1991) A new site for the activation of cardiac calcium channels defined by the nondihydropyridine FPL 64176. *J Pharmacol Exp Ther.* 259:982-987.
- Robina I, Moreno-Vargas AJ, Carmona AT and Vogel P (2004) Glycosidase inhibitors as potential HIV entry inhibitors? *Curr Drug Metab* 5:329-361.
- Shafiee-Nick R, Pyne NJ, and Furman BL (1995) Effects of type-selective phosphodiesterase inhibitors on glucose-induced insulin secretion and islet phosphodiesterase activity. *Br J Pharmacol* 115:1486-1492.
- Skasa M, Jungling E, Picht E, Schondube F, and Luckhoff A (2001) L-type calcium currents in atrial myocytes from patients with persistent and non-persistent atrial fibrillation. *Basic Res Cardiol* 96:151-159.
- Springborg J, Gromada J, Madsen P, Varming AR, and Fuhlendorff J (1997) Increase in $[Ca^{2+}]_i$ and subsequent insulin release from beta TC3-cells with the L-type Ca^{2+} -channel activator, FPL 64176. *Adv Exp Med Biol.* 426:149-157.
- Striessnig J, Murphy BJ, and Catterall WA (1991) Dihydropyridine receptor of L-type Ca^{2+} channels: identification of binding domains for $[^3H](+)$ -PN200-110 and $[^3H]$ azidopine within the alpha 1 subunit. *Proc Natl Acad Sci USA* 88:10769-10773.
- Usovich MM, Gigg M, Jones LM, Cheung CW, and Hartley SA (1995) Allosteric interactions at L-type calcium channels between FPL 64176 and the enantiomers of the dihydropyridine Bay K 8644. *J Pharmacol Exp Ther.* 275:638-645.
- Wiesner J, Mitsch A, Wissner P, Jomaa H, and Schlitzer M (2001) Structure-activity relationships of novel anti-malarial agents. Part 2: cinnamic acid derivatives. *Bioorg Med Chem Lett* 11: 423-424.
- Wollheim CB (2000) Beta-cell mitochondria in the regulation of insulin secretion: a new culprit in type II diabetes. *Diabetologia* 43:265-277.
- Yibchok-Anun S, Cheng H, Heine PA, and Hsu WH (1999) Characterization of receptors mediating AVP- and OT-induced glucagon release from the rat pancreas. *Am J Physiol* 277:56-62.

Zheng W, Rampe D and Triggle DJ (1991) Pharmacological, radioligand binding, and electrophysiological characteristics of FPL 64176, a novel nondihydropyridine Ca²⁺ channel activator, in cardiac and vascular preparations. *Mol Pharmacol* 40:734-741.